HANDLING ANALYSIS OF TRACKED AND WHEELED MILITARY VEHICLES

PALETLİ VE LASTİK TEKERLİ ASKERİ ARAÇLARIN MANEVRA ANALİZLERİ

FETİHHAN GÜRAN

ASSOC. PROF. DR S. ÇAĞLAR BAŞLAMIŞLI

Supervisor

Submitted to

Graduate School of Science and Engineering of Hacettepe University

As a Partial Fulfillment to the Requirements for the Award of the Degree of Master of Science in Mechanical Engineering.

2021

To my family.

ABSTRACT

HANDLING ANALYSIS OF TRACKED AND WHEELED MILITARY VEHICLES

Fetihhan GÜRAN

Master of Science Degree, Department of Mechanical Engineering

Supervisor: Assoc. Prof. Dr. S. Çağlar BAŞLAMIŞLI

Jun 2021, 69 pages

The aim of this thesis is to create a simulation environment that can model non-linear dynamics of tracked vehicles and wheeled vehicles including track-ground and tire-ground relations.

Firstly, three different tracked vehicles and two different wheeled vehicles have been modelled in MATLAB SIMULINK environment. The tracked vehicles are six, eight and ten road wheel vehicles, while wheeled vehicles are Ackermann steered and skid steered 6x6 wheeled vehicles. The dynamic models of tracked and wheeled vehicles differentiate in terms only tire and track; all the parameters of the hulls of the vehicles are the same. For traction force calculation, the flexible pad formula has been used for tracked vehicles and has been adopted to wheeled vehicles. Also, stability definitions that are available in the literature for linear and simple vehicle models have been implemented for all vehicles and, the transitions between neutral steer to understeer or neutral steer to oversteer behaviors have been represented for created non-linear vehicle models.

After the analysis it has been concluded that, for tracked vehicles, as the number of the road wheels increases the agility of the vehicle increases. Moreover, with this thesis parameter set, skid steering vehicles show oversteering behaviors whereas Ackermann

steering vehicle shows understeering behaviors. In addition to these, adopted flexible pad formula for wheeled vehicles performs coherent responses with the literature and reveals expected results.

Keywords: handling, tracked vehicles, skid steering, combined slip force generation,

ÖZET

PALETLİ VE LASTİK TEKERLİ ASKERİ ARAÇLARIN MANEVRA ANALİZLERİ

Fetihhan GÜRAN

Yüksek Lisans, Makina Mühendisliği Bölümü

Danışman: Doç. Dr. S. Çağlar BAŞLAMIŞLI

Haziran 2021, 69 sayfa

Bu tezin amacı; palet-zemin ve lastik-zemin ilişkilerini de içeren, paletli araçların ve 6x6 lastik tekerli araçların geçici rejim dinamiklerini modelleyebilen bir simülasyon ortamı yaratmaktır.

Öncelikle üç farklı paletli araç ve iki farklı lastik tekerli araç MATLAB SIMULINK'de modellenmiştir. Paletli araçlar altı, sekiz ve on yol tekerli, lastik tekerli araçlar Ackermann manevrası ve kızak manevrası yapan 6x6 araçlardan oluşmaktadır. Bu paletli ve lastik tekerli araçların dinamik modelleri teker ve palet olarak farklılaşmaktadır, araçların gövdelerinin özellikleri aynıdır. Çekiş kuvveti hesabı için esnek pabuç formülü paletli araçlarda kullanıldı ve lastik tekerli araçlara uyarlandı. Ayrıca tüm araçlar için literatürde bulunan, doğrusal ve basit araç modelleri için geçerli olan istikrar tanımlamaları ortaya konulmuştur ve yaratılmış olan doğrusal olmayan araç modelleri için nötr kaymadan önden kaymaya ve nötr kaymadan arkadan kaymaya davranış geçişleri gösterilmiştir.

Analizlerden sonra, paletli araçlarda yol tekerlerinin sayısı arttıkça aracın kıvraklığının arttığı sonucuna varılmıştır. Dahası, bu tezin değişkenleriyle, Ackermann manevrası yapan araç önden kayma davranışları gösterirken kızak manevrası yapan araçlar arkadan

kayma davranışları gösterirler. Bunlara ek olarak, lastik tekerli araçlara uygulanan esnek pabuç formülü literatüre uygun davranışlar vermiştir ve beklenen sonuçları göstermiştir.

Anahtar Kelimeler: manevra davranışı, paletli araçlar, kızak direksiyon, birleşik kayma kuvvet kazanımı

ACKNOWLEDGEMENTS

First of all, I would like to thank my supervisor, Assoc. Prof. Dr. S. Çağlar BAŞLAMIŞLI for his guidance and assistance during the entire graduate period. He consistently allowed this thesis to be my own work but steered me in the right direction whenever he thought I needed it.

I would like to thank Cantürk SANAN, Alperen KALE and Hazim Sefa KIZILAY who have been with me throughout the thesis as well as from the beginning of my university life and professional life and who supported me in all matters.

Finally, I present my endless gratitude to my wife, who made me come to these days, always with me and motivated me patiently under challenging times. Besides, I would also like to thank my mother, my father and my sisters, who helped me whenever I needed them.

TABLE OF CONTENTS

LIST OF FIGURES

LIST OF TABLES

LIST OF SYMBOLS & ABBREVIATIONS

Symbols

XYZ	Coordinate Axes of Ground Fixed Frame
xyz	Coordinate Axes of Body Fixed Frame
u	Longitudinal Velocity of the Vehicle in Body Fixed Frame
v	Lateral Velocity of the Vehicle in Body Fixed Frame
V	Velocity Vector of the Vehicle
β	Side Slip Angle
φ	Heading Angle
ψ	Yaw Angle
$F_{x,\ resultant}$	Resultant Forces on the Vehicle in x Direction
$F_{y,\ resultant}$	Resultant Forces on the Vehicle in y Direction
$M_{z,\ resultant}$	Resultant Moments on the Vehicle in z Direction
m	Mass of the Vehicle
I_z	Z Moment Inertia of the Vehicle
a_x	Longitudinal Acceleration of the Vehicle in Body Fixed Frame
a_y	Lateral Acceleration of the Vehicle in Body Fixed Frame
$\ddot{\psi}$	Yaw Acceleration of the Vehicle in Body Fixed Frame
r	Yaw Rate of the Vehicle
F_{xL}	Total Left Side Longitudinal Forces
F_{xR}	Total Right Side Longitudinal Forces
F_{xLi}	Left Side Longitudinal Force of i^{th} axle
F_{xRi}	Right Side Longitudinal Force of i^{th} axle
F_{aero}	Aerodynamic Force

F_{incl}	Weight Component of the Vehicle Horizontal to Inclination Plane
F_{roll}	Rolling Resistance
ρ	Density of Air
A	Frontal Area of the Vehicle
C_d	Drag Coefficient of the Vehicle
g	Acceleration of Gravity
θ	Inclination Angle
f_r	Rolling Resistance Coefficient
k_r	Rolling Resistance Coefficient
F_{zL}	Total Left Side Normal Forces
F_{zR}	Total Right Side Normal Forces
F_{zLi}	Left Side Normal Force of i^{th} axle
F_{zRi}	Right Side Normal Force of i^{th} axle
F_{yL}	Total Left Side Lateral Forces
F_{yR}	Total Right Side Lateral Forces
F_{yLi}	Left Side Lateral Force of i^{th} axle
F_{yRi}	Right Side Lateral Force of i^{th} axle
M_{FyL}	Total Moment on CG Created by Left Side Lateral Forces
M_{FyR}	Total Moment on CG Created by Right Side Lateral Forces
t	Track Width
x_i	Longitudinal Distance Between the CG and i^{th} Axle
$F_{st,i}$	Statically Distributed Load on i^{th} Axle
$\Delta F_{lon,i}$	Load Transfer Due to Longitudinal Acceleration on i^{th} Axle
$\Delta F_{lat,i}$	Load Transfer Due to Lateral Acceleration on i^{th} Axle
n	Number of Axles

h_{cg}	Height of the CG
k_i	Stiffness of the Spring on ith Axle
Δz_i	Relative Displacement Between Road Wheel and Vehicle Body
γ	Pitch Angle of the Vehicle Body
K_p	Pitch Stiffness of the Vehicle Body
L	Wheelbase
u_{Li}	Longitudinal Velocity Component under the ith Axle on the Left Side
u_{Ri}	Longitudinal Velocity Component under the ith Axle on the Right Side
v_{Li}	Lateral Velocity Component under the ith Axle on the Left Side
v_{Ri}	Lateral Velocity Component under the ith Axle on the Right Side
$\dot{X}$	X Component of Velocity in Ground Fixed Frame
$\dot{Y}$	Y Component of Velocity in Ground Fixed Frame
X	X Component of Location in Ground Fixed Frame
Y	Y Component of Location in Ground Fixed Frame
R_c	Radius of Curvature

Abbreviations

CG	Center of Gravity
ASWV	Ackermann Steered Wheeled Vehicle
SSWV	Skid Steered Wheeled Vehicle
6RWTV	Six Road Wheel Tracked Vehicle
8RWTV	Eight Road Wheel Tracked Vehicle
10RWTV	Ten Road Wheel Tracked Vehicle

1. INTRODUCTION

1.1 State of the Subject

There have been many studies on the lateral non-linear dynamics of the wheeled ground vehicles. Compared to the wheeled vehicles, there are significantly less studies on tracked vehicles non-linear lateral dynamics analysis. So, in this thesis, it has been aimed to create non-linear tracked vehicle models and compare them with the previous works in the literature and wheeled vehicles of the same size.

In the conceptual design phase of a vehicle, it is critical to investigate driving performance in terms of stability and handling in order to obtain optimum vehicle parameters for motor, transmission, suspension systems. Therefore, the vehicle must be modeled and analyzed with all its dynamics. The results of these calculations lead to verify designed geometries and sub-systems. Especially, for the tracked vehicles, lateral dynamics bear an important role for motor selection since some skid steering maneuvers require a great amount of power. As the lateral acceleration increases the demanded engine power reaches power limits shown below *Figure 1*.

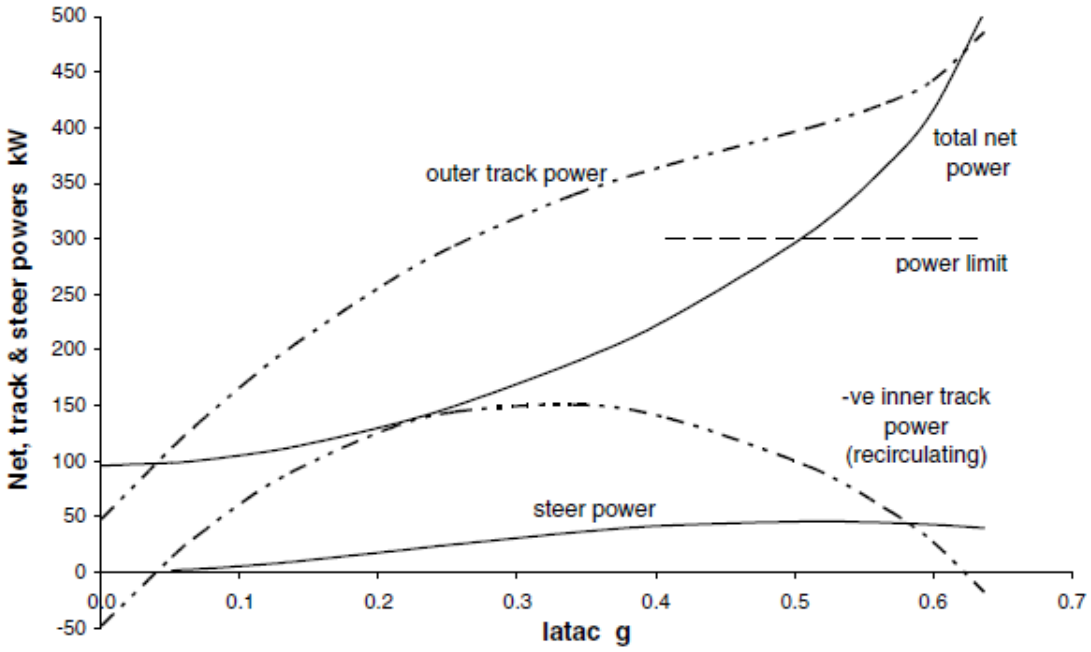

Figure 1. Inner and outer sprocket powers and steer power.[1]

There are little to no data about tracked vehicle understeer, neutral steer and oversteer definitions in the literature. In this study, these definitions have been deduced depending on the similar literature for wheeled skid steered vehicles and calculated. Steady state analysis possesses an important aspect of the understanding of the vehicle horizontal plane motions. Determining stability characteristics of a vehicle has been useful to design the vehicle in the desired way. According to results geometry of the vehicle, position of the axles with respect to center of gravity etc. can be decided. In this study, these stability definitions have been deduced, depending on the similar literature for wheeled skid steered vehicles, and calculated.

Creating a simulation environment that simulates different vehicles of the same size will give valuable insights about vehicle design. In this simulation environment the vehicle models differentiate in traction generation method (track/ tire) from the ground. Together with the above considerations, simulation environment with fast execution time has been created and a detailed analysis has been made for five different vehicles (Ackermann steered wheeled, skid steered wheeled, six road wheel tracked, eight road wheel tracked and ten road wheel tracked).

1.2 Scope of the Thesis

In this study non-linear dynamic models for 6x6 front wheel steered, 6x6 skid steered wheeled vehicles and six, eight and ten road wheel tracked vehicles have been created similar to tracked vehicle model of Galvagno, Rondinelli and Velardocchia [2] with the use of the flexible pad formula defined by Maclaurin [1], and this formula adapted to wheeled vehicles. To make a valid comparison; same longitudinal, lateral and vertical dynamics applied to all models and force generation for track pads using flexible pad formula adapted to tire dynamics for wheeled vehicles.

Simulations have been carried out to fully understand the steady state behaviors of the vehicles and compared with the literature to verify the models. Lateral coefficient of friction

curves and sprocket torques corresponding to different turn radii have been calculated for tracked vehicles. These outcomes have been compared with the Wong and Chiang's [3] results. For steady state analysis, yaw rate gains and radius of curvature gains have been obtained with the definitions of stability factors for every vehicle.

After the above explained studies were conducted and valuable outcomes of the analyses were gathered. It was observed that, for tracked vehicles, as the number of road wheels increase, the agility of the vehicle increases. So, tracked vehicles with more number of road wheels require less amount of steering input to make same turn radius at the same speed. Another important outcome is, calculating all of the vehicles stability characteristics using the available approaches in the literature for linear and simplified vehicle models [5][6] as neutral steer and, experiencing neutral steer to understeer and neutral steer to oversteer vehicle behavior transitions after certain speeds. The vehicle models in this thesis are non-linear so, experiencing these transitions are due to non-linearity.

In this thesis, the main contribution is, creating a fast executing simulation environment that can handle non-linear dynamics of tracked and wheeled vehicles and adopting the flexible pad formula for wheeled vehicles, that is created for tracked vehicles.

1.3 Outline of the Thesis

This thesis is composed of five main parts. In the first part, an overview of the concept of the thesis has been given. After that, an adequate literature background has been given.

In the literature review section, the subject has been divided to two parts. In the first part vehicle dynamics studies are investigated for both tracked and wheeled vehicles. In the last part traction and lateral force generation calculation methods have been given in detail for both track pads and tires.

The mathematical modelling of the all five vehicles has been represented in modelling section. All of the vehicles have some common motion dynamics like longitudinal, lateral and yaw motions, weight transfers due to vehicle body motions etc. These calculations have been explained in an integral manner. Longitudinal slips and slip angles under each wheel, traction and lateral force generations under each wheel etc. have been studied separately for tracked and wheeled vehicles. Also, the stability analysis for the tracked and wheeled vehicles have been given in this section.

In the simulations and results section, handling analysis through SIMULINK has been explained. Each of the vehicles has been subjected to various scenarios such as point turn and constant radius turn maneuvers etc. These scenarios have been presented in detail and the outcomes have been investigated.

All of the conclusions from tens of simulations and mathematical calculations have been discussed in the conclusion and future works sections. Also, what can be done in order to improve the studies in relative field has been explained. The presumed future works have been discussed in this section.

2. LITERATURE SURVEY

In this section, previous works related to the subjects mentioned in this thesis has been investigated. The literature survey is composed of mainly two parts. These are the vehicle dynamics and track-ground/ tire-ground relations.

2.1. Vehicle Dynamics

Vehicle dynamics has been studied as long as the vehicles exist. The literature about the vehicle dynamics has been given in two different sections for wheeled and tracked vehicles.

2.1.1 Wheeled Vehicle Dynamics

Jazar [7] has examined the dynamics of the wheeled vehicles in detail. He has explained stability factor Equation (2.1) and related understeer, neutral steer and oversteer behaviors of wheeled vehicles for steady state analysis. These behaviors are related to sign of the stability factor. If the sign of the stability factor is positive the vehicle is understeer and to keep a constant turning circle steering wheel angle must be increased for increasing vehicle speeds. If the sign of the stability factor is negative, the vehicle is oversteer and to keep a constant turning circle steering angle must be decreased for increasing vehicle speeds. These stability definitions are valid for linear and simple vehicle models. Regarding this thesis, these definitions have been derived and calculated, but they are only valid for slow speeds. After certain speeds vehicles started to show neutral steer to understeer or neutral steer to oversteer behavior transitions. The stability factor is given below:

$$K = \frac{m}{l^2}\left(\frac{a_2}{C_{\alpha f}} - \frac{a_1}{C_{\alpha r}}\right) \tag{2-1}$$

where K is the stability factor, m is vehicle mass, l is the wheel base, a_1 and a_2 are the front and rear axle distances to CG respectively and $C_{\alpha f}$ and $C_{\alpha r}$ are the front and rear tire cornering stiffnesses respectively.

At the critical speed the response of the vehicle is no longer related to steering angle and in theory it can take any possible curvature and therefore the vehicle is unstable. If the stability factor is zero, the vehicle is neutral steer and to keep a constant turning circle steering angle must not be changed (*Figure 2*).

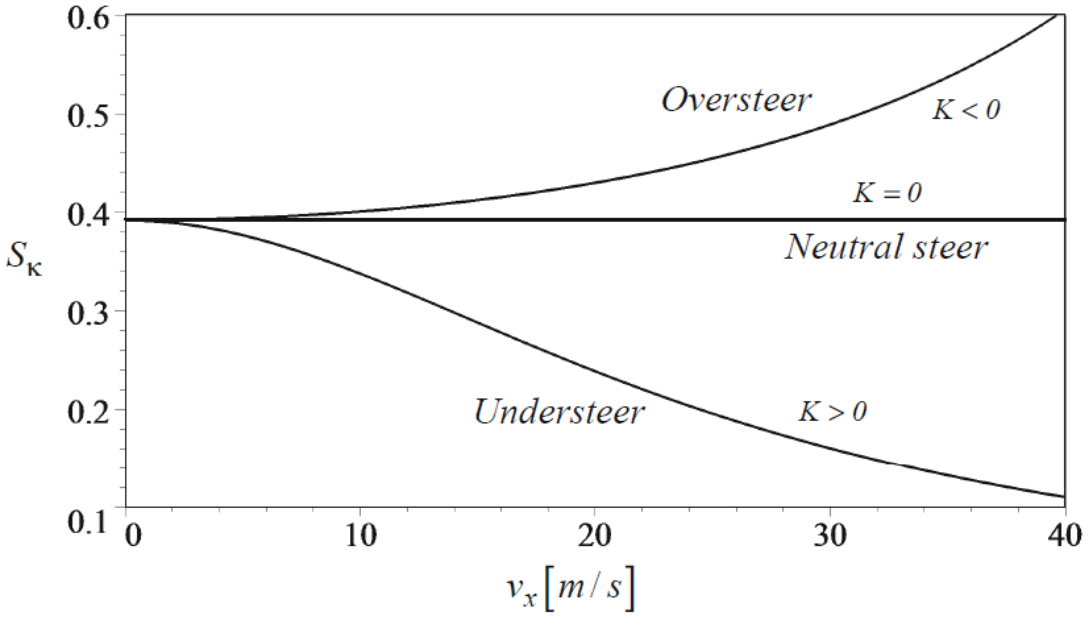

Figure 2. Comparison of the curvature response for a car with oversteer, neutral steer and understeer behaviors.[7]

Bayar [5] has developed a general non-linear model for multi-axle steered vehicles in full body dynamics motions. The sprung mass motions and unsprung mass motions are included with rolling dynamics of the wheels. The unsprung mass motions are only in vertical direction, but sprung mass has been investigated with roll, pitch and vertical directions.

In this work different steering strategies have been applied to two, three and four axle vehicles. In these strategies different axles are steered and results are recorded. It has been concluded that steering the intermediate axles to reasonable levels helps to increase yaw velocity response without losing from vehicle side slip angle. For the understeer, oversteer and neutral steer behavior of the vehicles, a simplified and linear approach has been used. These identifications have been derived from two axle vehicle and have been extended to three and four axle vehicles.

Pacejka [8] has investigated tire force generation mechanics and vehicle handling planar dynamics. His study regarding the tire force generation mechanics will be explained in detail in the upcoming sections. For vehicle planar dynamics a linearized and simple model has been built. Similar to conducted study in [7], a constant forward velocity assumed and decoupled from the system of equations. Also roll angle and its derivative have been set to zero and roll dynamics decoupled from the system of equations. Conversely in this thesis these simplifications have not been used and non-linear models of the vehicles have been built.

Ni, Hu and Li [6] have created two 8x8 wheeled vehicle models, one for Ackermann steered vehicle and one for skid steered vehicle. The main parameters like the total mass, the distance of each axle to the center of mass, the track width, the stiffness of each tire and the yaw inertia for two vehicles are same. In the vehicle models, some assumptions have been made:

- The vehicle is assumed to move on a plane surface,
- The vertical displacement of each wheel is neglected,
- The center of mass is located at the center of geometry,
- The longitudinal slip is limited to 0.1 and the slip angle is limited to 5^{o}.

The test results have been compared with the simulation results and the results have seem to coincide with each other.

The comparison of the skid steered and Ackermann steered vehicles has been investigated in three parts namely, steady state response, transient response and worn of tires. For steady state response analysis stability factor for four wheel vehicles has been introduced and extended to eight wheel Ackermann steered vehicle and eight wheel skid steered vehicle. Then yaw rate, curvature and side slip gains have been plotted against vehicle speed. From yaw rate gain curves, it has been concluded that, skid steer vehicle has lower yaw rate gain and the relation between yaw rate gain and the speed is more linear than Ackermann steered vehicles which indicates that skid steered vehicle has a better handling behavior. Similar to yaw rate gain curvature gain is always lower for skid steered vehicles which means skid steered vehicles take larger radii at the same vehicle speed.

2.1.2 Tracked Vehicle Dynamics

Kitano and Kuma [9] have developed a transient model of a tracked vehicle for plane motion. The inputs to the system were both track velocities. Some assumptions have been made in order to simplify the model:

- The road wheels were arranged in tandem on each side of the hull and possessed independent suspensions with same spring rates.
- The vehicle was geometrically symmetric with respect to xz-plane and yz-plane.
- The vehicle load was concentrated under road wheels.
- There was anisotropic Coulomb friction between ground and track pad and aerodynamic forces were neglected

The force generation equation used in [9]:

$$F_x = F_N E_1 (1 - e^{-E_2|S|}) \cos(\psi + \pi) \qquad (2\text{-}2)$$

where F_N is the normal force, S is the slip, ψ is the angle that determines the direction of slipping, E_1 and E_2 are the positive constants that are determined by pull-slip tests.

The simulations have been carried out for three different vehicle speeds, 6 m/s, 8 m/s and 10 m/s. To realize the maneuver the speed of the inner track was reduced to half in 3 seconds *Figure 3*.

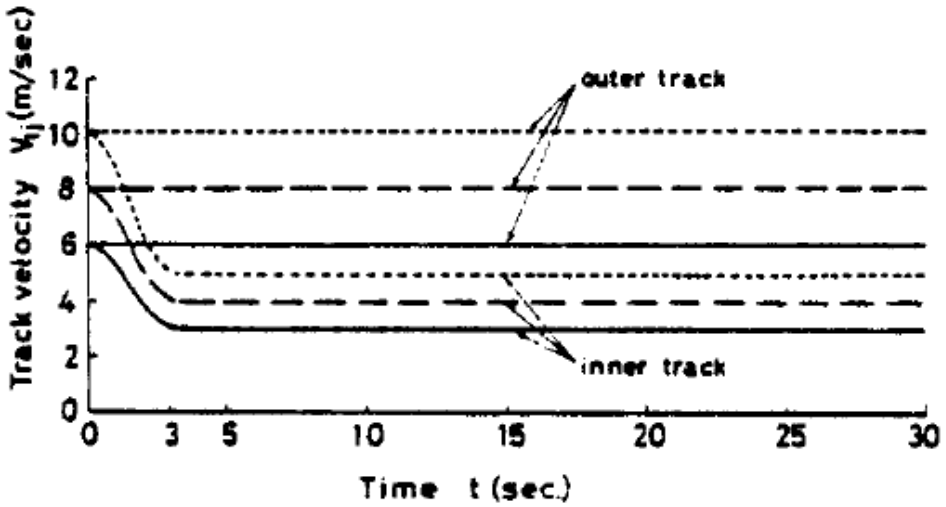

Figure 3. Track speeds vs time.[9]

The outcomes of the simulations have been analyzed and a strong dependence between vehicle speed and steering input have been noticed. When the initial velocity of the vehicle is higher than 8 m/s, radius of curvature drops sharply and vehicle oversteers.

Galvagno, Rondinelli and Velardocchia [2] have built a dynamic electromechanical transmission model and a non-linear transient tracked vehicle model for series hybrid vehicles. These models have been created to describe power flows for required maneuvers and energy regeneration capacities. In this work same simplifications have been made as Kitano and Kuma's [9] study but aerodynamical forces have not been neglected and road inclination has been included into model. Track-ground relations have been described as a hyperbolic tangent function of Coulomb friction and threshold values are set 30° for slip angle and 0.3 for longitudinal slip. Load transfers due to roll and pitch motions of the vehicle hull has been included and defined.

Transient and steady state analyzes have been executed to calculate required powers from propulsion and steering motors. The step steer input has been applied while the vehicle was travelling at 36 km/h straight. Required torque values for this maneuver have been calculated and power requirements have been designated. The need of power for two sides of the tracked vehicle has been plotted for steady state motions against radius of curvature.

2.3 Tractive Force Generation

The tire-ground and track-ground relations regarding the force generation has been one of major areas for vehicle handling studies. All ground vehicles other than rail vehicles generate the force via a rubber medium between the ground and vehicle body for the required motion. This rubber medium deflects and makes a relative motion between ground and vehicle body through slipping. This slipping in any direction creates force.

2.3.1 Tire-Ground Relation

Bakker, Nyborg and Pacejka [10] have developed a formula to describe the tire behavior in pure cornering and pure braking conditions. The formula has been based on measured data from test results. The formula is able to define side force, brake/ traction force and self-aligning torque. However, the application of the formula is only valid for steady state conditions and it forms the basis for combined movement situations. This study has paved the road for the prominent tire theory called the "Magic Formula" which will be examined later in this section.

Dugoff, Fancher and Segel [11] have made analyses to investigate the effect of tire characteristics to a vehicle requiring combined longitudinal and lateral forces. Four different types of scenarios have been examined, a steady state turn, braking during a steady state turn, increasing steering angle while undergoing severe lateral acceleration and combined lane change with braking. In these analyses cornering stiffness of the tire, braking stiffness of the tire and coefficient of friction between the tire and ground have been altered to examine their effect on maneuvers.

Pacejka and Bakker [12] have improved their previous work [10] including combined slip conditions. With this study the formula has been officially started to be called as "The Magic Formula". The formula is capable of describing tire lateral force, tire longitudinal force and self-aligning torque for both pure slip and combined slip conditions. The Equation (2.3)shows the formula for pure slip conditions. The combined slip results are gathered using Equation (2.3) with lengthy set of extensions of normalized combined slips in [12].

$$y(x) = D\ sin[C\ \arctan\{B\ x - E(B\ x - \arctan(B\ x))\}] \quad (2.3)$$

where *B*, *C*, *D* and *E* are dimensionless stiffness, shape, peak and curvature coefficients.

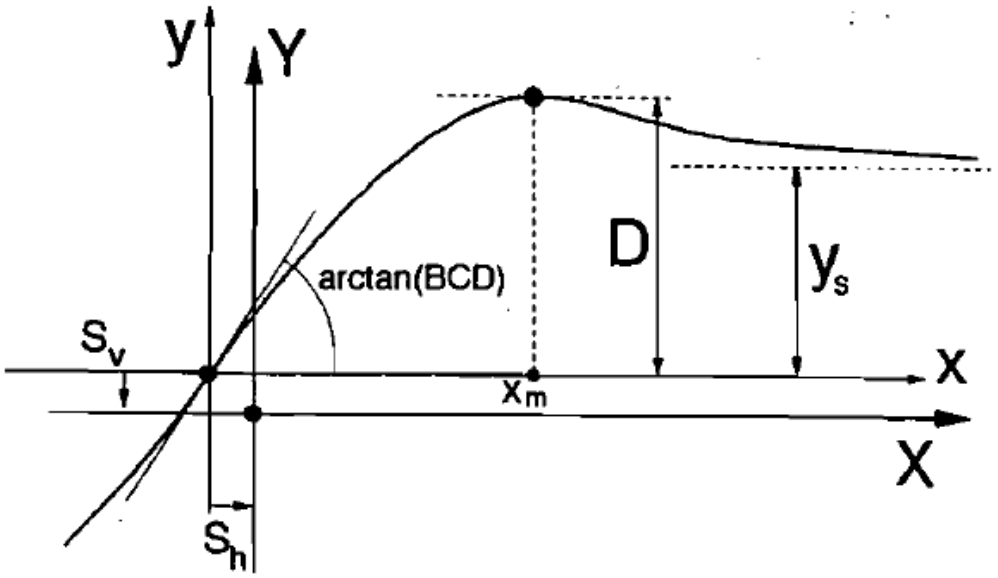

Figure 4. A typical characteristic indicating the meaning of some of the coefficients of formula. [12]

2.3.2 Track-Ground Relation

Steeds [13] performed one of the first research studies about tracked vehicles. In this work the track pad ground relation has been assumed as a Coulomb friction which takes place in between.

Wong [14,15] has proved experimentally that the shear stress generated under the track pad depends on the shear displacement. Accordingly, the shear stress reaches its maximum value after a particular value of shear displacement occurs as seen in *Figure 5*. Shear displacement is the travelled distance of a particular point under the track pad from the initial point of contact, during a finite interval of time with a sliding velocity. The sliding velocity is the relative velocity of a point under the track pad and in contact with the ground, with respect to ground. The sliding velocity and shear displacement can be expressed as [3]:

$$V_{t_1 j} = V_{o_1 y_1} - r\omega_o \tag{2.4}$$

$$j = \int_0^t V_{t_1 j}\, dt \tag{2.5}$$

where $V_{t_1 j}$ is the sliding velocity of point o_{t_1}, $V_{o_1 y_1}$ is the absolute velocity of o_1 in the y_1 direction, r is the radius of the sprocket, ω_o is the angular velocity of the sprocket and j is the shear displacement. A detailed geometric and kinematic representation can be seen in *Figure 6*.

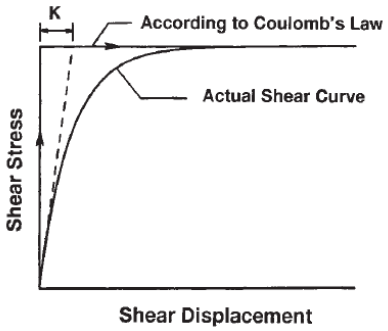

Figure 5. Comparison of the measured field data and Coulomb's Law.[3]

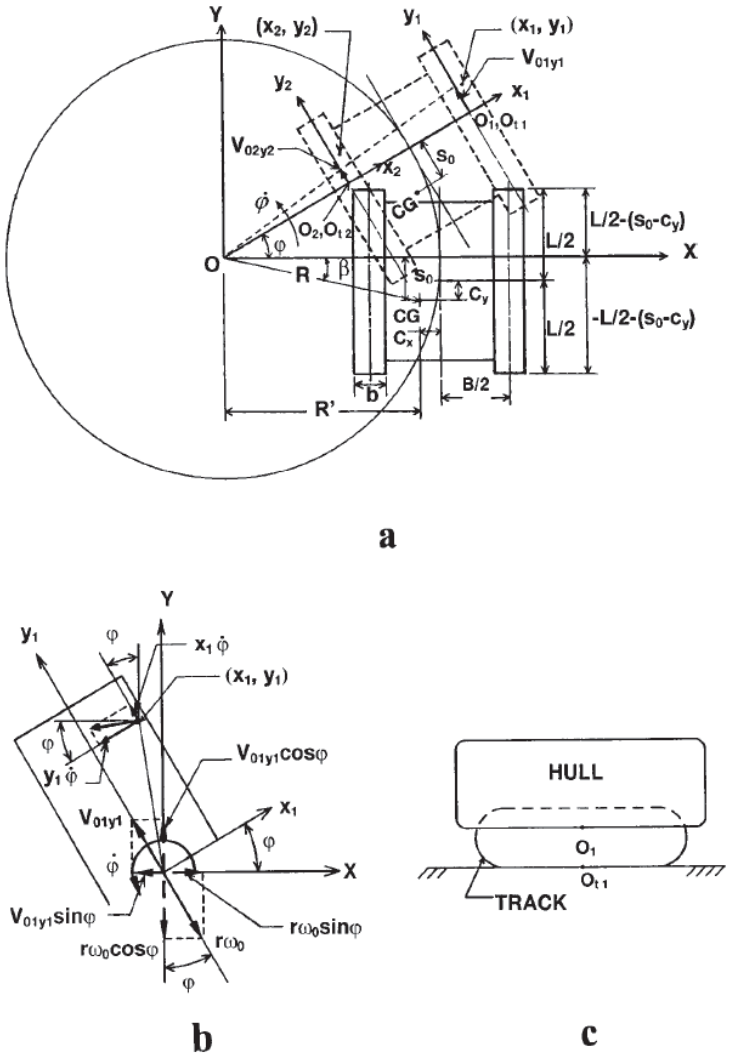

Figure 6 Geometric and kinematic relations of a track element during a turning maneuver [3].

Wong and Chiang [3] developed a general theory for tracked vehicles. The theory majorly depends on the previously explained difference between Coulomb's Law and shear stress shear displacement relation. In this work a mathematical model for a tracked vehicle has been build. The following assumptions have been made:

- The ground is firm.
- The direction of the shear stress is opposite to direction of the sliding velocity.

The mathematical model has been executed for a particular vehicle and the results compared with the experiments. Some of the presented results were sprocket torque vs turn radius and lateral coefficient of friction vs turn radius *Figure 7-Figure 8*. The general theory showed a strong consistency with measured field data.

The shear stress and shear force developed on the track pad due to shear displacement [3]:

$$\tau = p\mu(1 - e^{-j/\kappa}) \tag{2.6}$$

$$dF = \tau dA \tag{2.7}$$

where p is the normal pressure, μ is the coefficient of friction and κ is the shear deformation modulus.

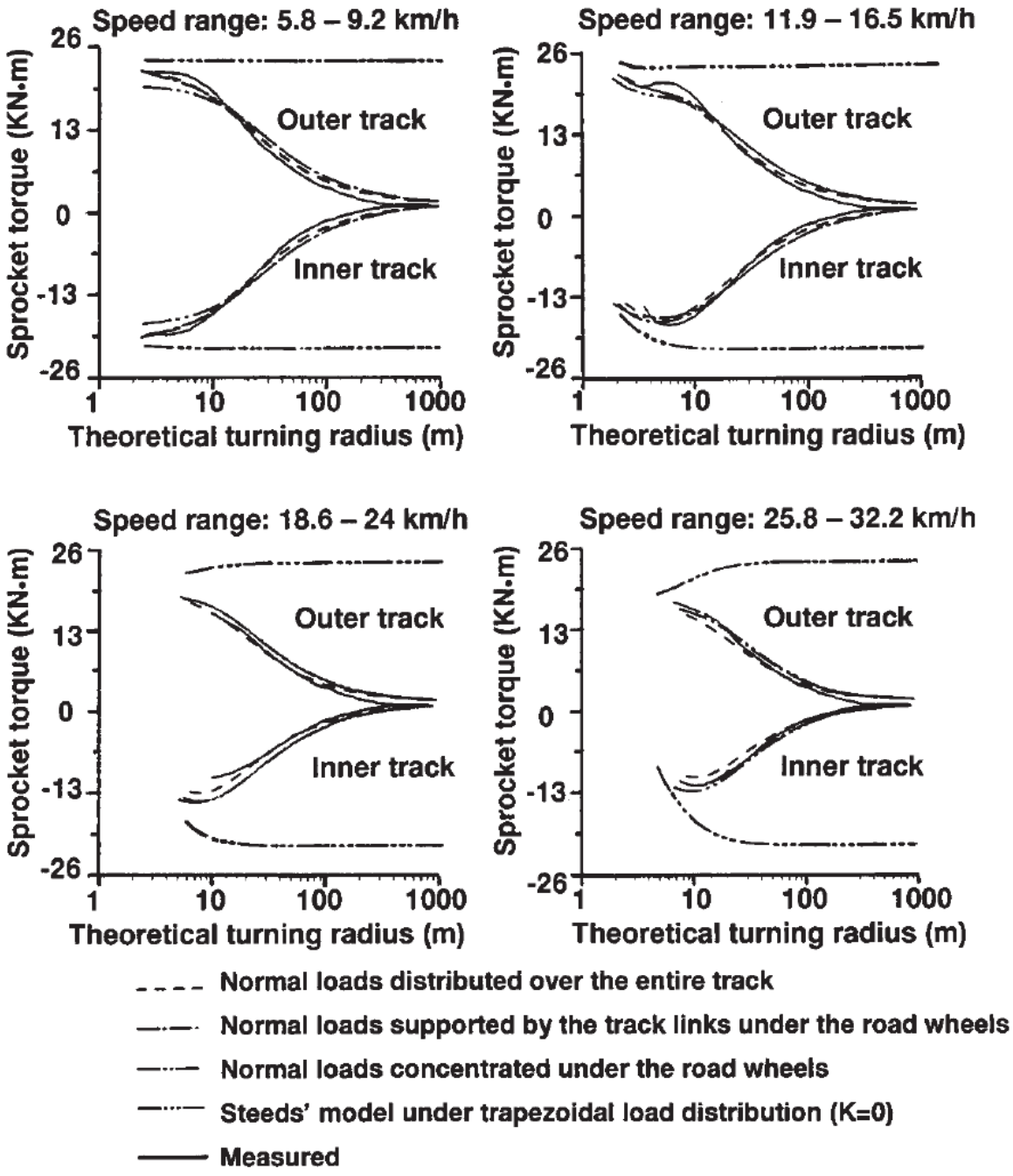

Figure 7. Sprocket Torques vs Turn Radius[3].

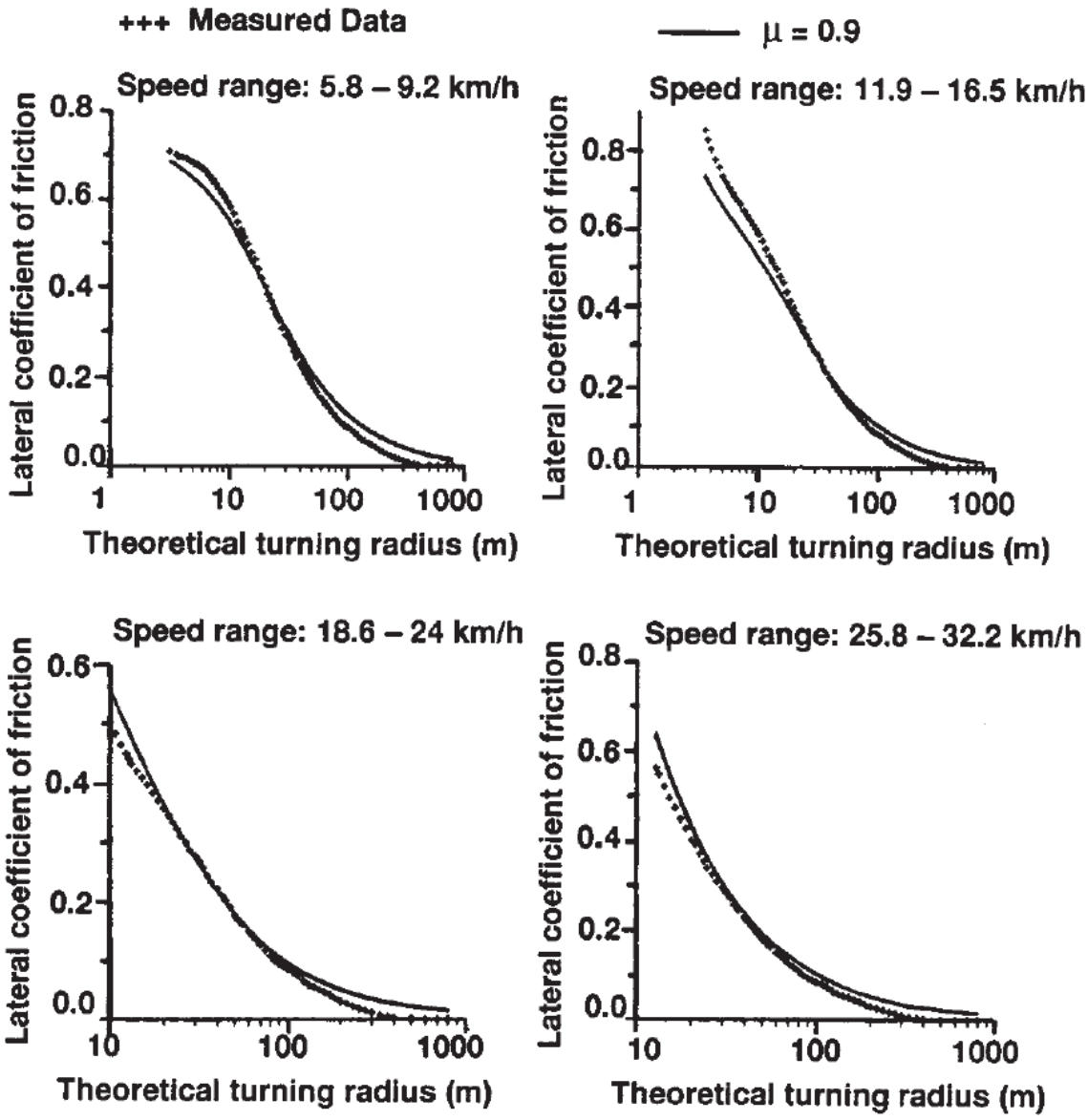

Figure 8. Lateral Coefficient of Friction vs Turn Radius[3].

Ehlert, Hug and Schmid [16] have conducted tests on PAISI (Power and inertia simulator) system where tracked vehicles are tested dynamically at the Automotive Institute, University of Federal Armed Forces, Hamburg. All of the resistances can be simulated on PAISI, including the turning resistance. The cornering effort is the major cause of the high propulsion in tracked vehicles. Therefore, the simulations and tests to analyze cornering resistances are essential.

In order to control of the test and validation of the models some analytical models have been analyzed and compared. These analytical models are Hock [17], IABG and Kitano [9,18] models. Among these models the simplest is the Hock model in which load transfers have not been calculated. But, both IABG and Kitano [9,18] models involve load transfers too. Kitano [9,18] model is the most sophisticated model however, it is also the most time consuming model. So, it is not suitable to use with PAISI system as stated in [16]. All of these three models have been modified and extended regarding the considerations included in the work of Ehlert [19]. Ehlert [19] considered the relation between internal losses and turn radius. With all of the above considerations, they concluded that, the Hock model with the extension of Ehlert's work is simple and gives reliable outcomes for steady state cases to calculate sprocket torques and lateral coefficient of friction. Furthermore, the IABG model with extension of Ehlert's work gives fast and reliable outputs for transient cases to calculate sprocket torques and lateral coefficient of friction.

The general theory of Wong [3] suggests using calculated moments of turning resistances $M_{T,}$ for lateral coefficient of friction. Because, there is uncertainty if empirical relations to calculate lateral coefficient of friction in [16] can be applied generally, stated in [3].

The lateral coefficient of friction μ_w can be calculated as:

$$\mu_w = \frac{WL}{4M_T} \tag{2.8}$$

where W is vehicle weight, L is track contact length and M_T is the total turning resistance moment due to lateral forces.

Maclaurin [1] has developed a flexible track pad model for skid steered tracked vehicles. The model is basically similar to Wong and Chiang's [4] general theory since it accounts for shear stiffness of the rubber track pad. The model has been fitted to experimental data and adopted to combined slip. Assuming that lateral and longitudinal slips constitute a resultant

slip vector. The lateral and longitudinal slips are the lateral and longitudinal components of this vector so that combined force distributed respectively. The created model showed good agreement with the field data.

The flexible pad formula is expressed as follows [1]:

$$F_R = 0.94\mu F_N(1 - e^{-10.7s}) \tag{2.9}$$

where F_R is the resultant tractive force, μ is the coefficient of friction, F_N is the normal force and s is the resultant slip vector.

$$s = \sqrt{s_l^2 + \tan^2 \alpha} \tag{2.10}$$

where s_l is the longitudinal slip and α is the slip angle.

$$F_X = \frac{s_l}{s} F_R \tag{2.11}$$

$$F_Y = \frac{tan\alpha}{s} F_R \tag{2.12}$$

The slip angle and the longitudinal slip are implemented in the flexible pad formula by carrying out shear displacement calculations as explained below:

The track pad is considered in transverse slices that are *dx* long as seen in Figure 9. So, the transverse shear force acting on this slice, when an α degree of slip angle exists, is:

$$f_y = k_s x \tan \alpha \, dx \tag{2.13}$$

Then the total lateral force:

$$F_y = k_s \tan\alpha \int_0^c x dx = k_s \left[\frac{x^2}{2}\right]_0^c = k_s \frac{c^2}{2} \tan\alpha \quad (2.14)$$

where k_s is the shear stiffness per meter of the rubber pad, x is the distance between the slice and the front of the pad, c is the length of the track pad and $x \tan\alpha$ is the shear deformation in transverse direction of the track pad.

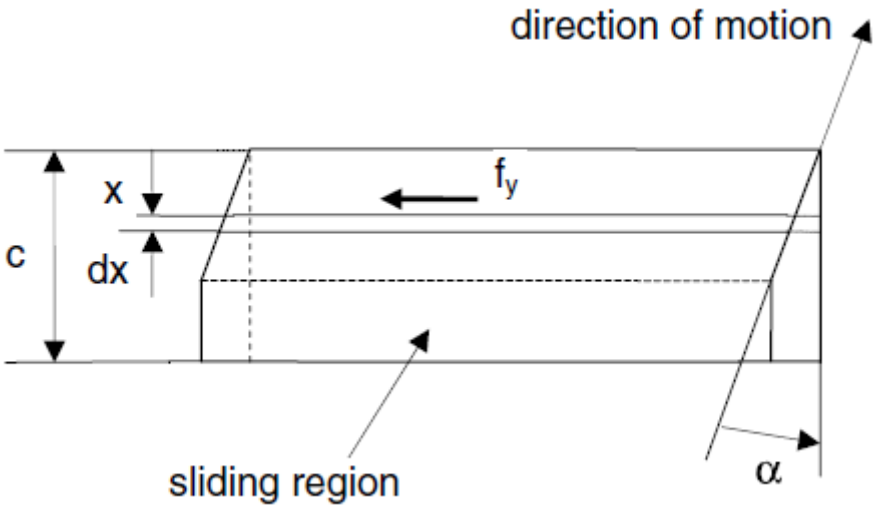

Figure 9 Track pad exposed to a slip angle of α [1].

The shear displacement, that is on the slice in longitudinal direction, is due to difference between wheel hub velocity and track velocity as seen in *Figure 10*. And can be expressed as below:

$$\delta_x = (V_t - V_v)t \quad (2.15)$$

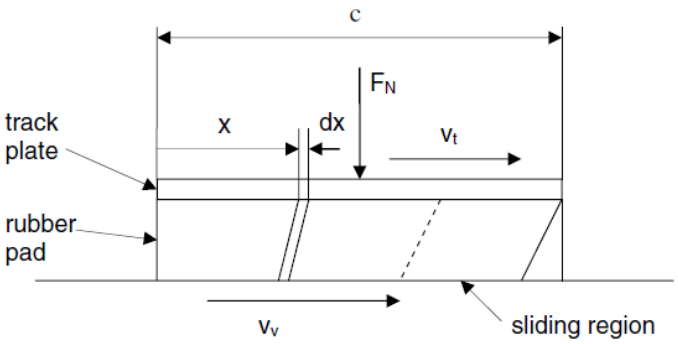

Figure 10 Cross section of a track pad during traction [1].

where V_t is the track velocity, V_v is the whel hub velocity and time t can be expressed as:

$t = \frac{x}{V_t}$ and δ_x becomes:

$$\delta_x = \frac{(V_t - V_v)}{V_t} x \tag{2.16}$$

where $\frac{(V_t - V_v)}{V_t}$ is the longitudinal slip s_t, so the tractive force on the slice:

$$f_x = \delta_x k_s dx = s_t k_s x dx \tag{2.17}$$

And total tractive force under the track pad:

$$F_{xt} = s_t k_s \int_0^c x dx \tag{2.18}$$

For combined slip, the resultant force vector becomes:

$$F_R = (s_t^2 + \tan^2 \alpha) k_s \int_0^c x dx \tag{2.19}$$

Maclaurin conducted above calculations for various cases and he fitted an exponential curve to data and gathered flexible pad formula as stated in Equation (2.9)

Maclaurin [20] has predicted steering performance of tracked vehicle by adopting the Magic Formula. During implementation, the Magic Formula needs characteristic constants for particular tire. In this work, these constants were gathered from available data for rubber track pad and adapted to the Magic Formula.

In this thesis the flexible pad formula has been used for tracked vehicles and it has been adopted to be used in wheeled vehicles to make a comprehensive comparison. For tracked vehicles, Coulomb friction based formulas exist in the literature [13]. In the coulomb friction based formulas the friction moment remains constant as the turn radius increases. But, in reality the experimental results show that as the turn radius increases the required sprocket torques differences decreases as seen in *Figure 7*.

In [1] a comparison between the flexible pad formula and Merritt/Steeds model (a coulomb friction based model) has been made as seen in *Figure 8*.

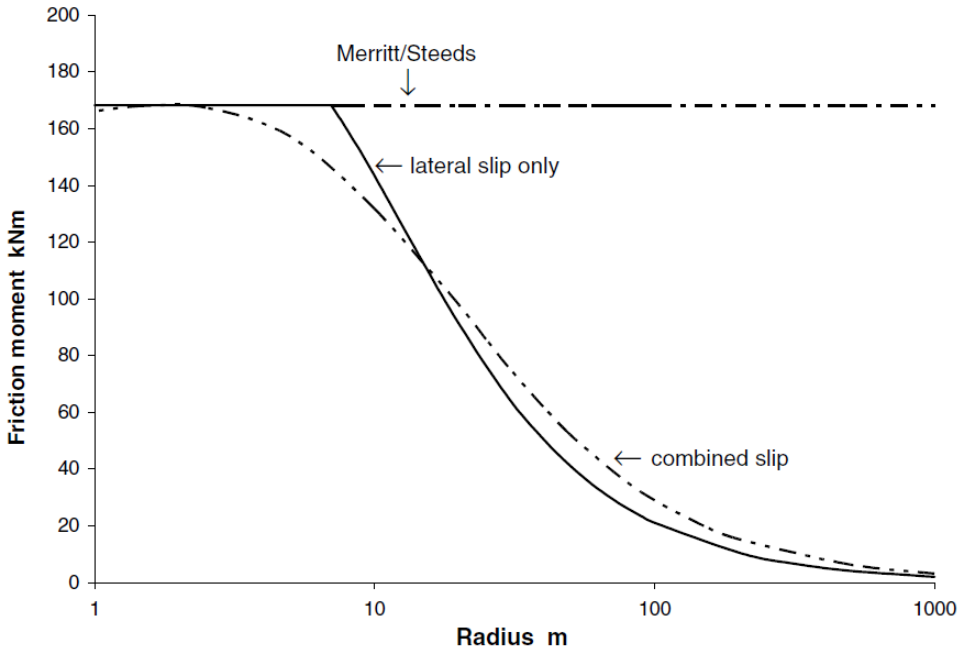

Figure 11 Friction moment comparison between Merritt/Steeds model and the flexible pad model [1].

The reason that the friction moment decreases as the turn radius increases is due to rubber flexibilities [1]. Wong's general theory [3] and Maclaurin's flexible pad formula [1] methods are accounting these flexibilities by taking into account the shear stiffness of rubber. Because of the considerations of these flexibilities, these models are capable of representing the real world behavior of skid steering vehicles when taking big turn radii.

Also, it can be seen in *Figure 7*, that the Steeds [13] method shows constant sprocket torques throughout the various radii, which is contrary to reality.

Despite the general theory of Wong and flexible pad formula of Maclaurin coincide in the base of track pad flexibilities, they differ from inputs to these formulas as shear displacement and slip since Maclaurin has fitted a curve to the flexible formula that is dependent to slip. But, in the base of flexible pad formula of Maclaurin the shear displacements are also used as in general theory of Wong, as explained detailly in Equations (2.13-2.19).

2.4 Tracked Vehicle Model Comparisons

In the previous sections, some of the literature studies have been given for tracked vehicle dynamics and tracked vehicle force generation methods. Here a neat and a simple table has been prepared in order to improve the understanding of the conducted work in *Table 1*.

Table 1 Tracked Vehicle Model Comparisons

Vehicle Models / Parameters	The model used in this thesis	Kitano and Kuma's Model [9]	Wong and Chiang's model [3]	Galvagno, Rondinelli and Velardocchia's Model [2]
Model Degree of Freedom	3	3	3	3
CG Location	Geometrically symmetric	Geometrically symmetric	Off from the geometric center	Off from the geometric center
Normal Load Distribution	Concentrated loads under the road wheels	Concentrated loads under the road wheels	• Concentrated loads under the road wheels • Loads supported only by the track links just right under the roadwheels • Loads distributed over the entire track	Concentrated loads under the road wheels
Ground Type	Firm Ground	Firm Ground	• Firm Ground	Firm Ground

Resistive Forces	• Aerodynamics Forces • Rolling Resistances • Inclination Forces	• Rolling Resistances	• Rolling Resistances	• Aerodynamics Forces • Rolling Resistances • Inclination Forces
Rolling resistance formula	$F_z(f_r + k_r V)$	$F_z f_r$	$F_z f_r$	$F_z(f_r + k_r V^2)$
Weight Transfers	Weight transfers due to roll and pitch motions of the body included	Weight transfers due to roll and pitch motions of the body included	Weight transfers due to roll and pitch motions of the body included	Weight transfers due to roll and pitch motions of the body included
Force generation formula (Long./ Lat.)	$0.94\mu F_N(1 - e^{-10.7s})$	$F_N E_1(1 - e^{-E_2\lvert S\rvert})\cos(\psi + \pi)\cos$ $F_N E_1(1 - e^{-E_2})\sin(\psi + \pi)$	$p\mu(1 - e^{-j/\kappa})dA$	$k\mu F_N tanh(\frac{3s_i}{s_{Fmax}})$ $k\mu F_N tanh(\frac{-3\alpha_i}{\alpha_{Fmax}})$
Input to force generation formula	Slip/ Slip Angle	Slip and direction of slipping	Shear displacement	Slip/ Slip Angle

3. MODELLING

3.1. Introduction

For the purpose of this thesis, nonlinear dynamics of five different vehicles have been modelled. Two of the vehicles are 6x6 wheeled vehicles. One vehicle executes maneuvers via Ackermann steering and will be named as Ackermann Steered Wheeled Vehicle (ASWV) while the other wheeled vehicle executes maneuvers via skid steering and will be named as Skid Steered Wheeled Vehicle (SSWV). The other three vehicles are tracked vehicles, one with six road wheels which will be named as 6 Road Wheeled Tracked Vehicle (6RWTV), one with eight road wheels which will be named as 8 Road Wheeled Tracked Vehicle (8RWTV) and one with ten road wheels which will be named as 10 Road Wheeled Tracked Vehicle (10RWTV) *Figure 12*. The main parameters like vehicle weight, track width and wheelbase are the same for all of the vehicles.

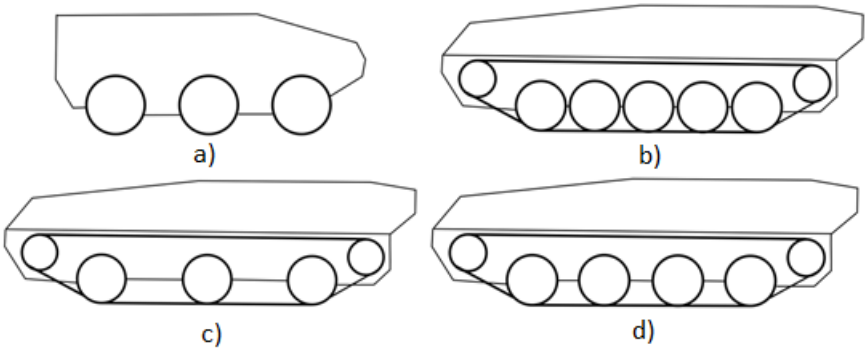

Figure 12. Tracked and Wheeled Vehicles. a) Both Ackermann Steered and Skid Steered Wheeled Vehicles b) Ten Road Wheel Tracked Vehicle c) Six Road Wheel Tracked Vehicle d) Eight Road Wheel Tracked Vehicle

Garber and Wong [21] conducted analyzes to assess pressure distribution under tracks. It has been concluded that assuming concentrated loads under road wheels is mostly fair. The 6RWTV is not a common practice for the vehicle of this size, because the main aim of tracked vehicles is to distribute the vehicle weight to the ground as much evenly as possible. The assumed vehicle mass is 30 tons. But it is a transition stage between a normal tracked vehicle and a 6x6 wheeled vehicle for a thorough comparison. As the load of the tracked vehicle is concentrated under road wheels and having the same major parameters as given before, there is no difference between the 6RWTV and SSWV. For

a tracked vehicle the longitudinal slips are the same for all of the track pads under the road wheels at the same side. This is also the case for a skid steered wheeled vehicle in this study. The detailed calculation will be given in sections to come. Furthermore, the tire ground and track pad ground relations have been resembled by using same theory, the flexible pad theory of Maclaurin [1].

The stability definitions of a Ackermann steered wheeled vehicle are well established as understeer, neutral steer and oversteer. Using the bicycle model, these definitions have been gathered for linear situations [7,14]. Also, for non-linear situations such as high vehicle speed and high lateral accelerations, the transitions between vehicle behaviors have been investigated and studied [14]. These vehicle behaviors are understeer, neutral steer and oversteer behaviors. But these stability definitions haven't been made for tracked vehicles. A simple method has been deduced from [5] and [6] and these definitions are established. In addition to these, the vehicle behavior transitions also investigated as the speed of the vehicle increases.

3.2. Assumptions

The following assumptions have been made for all of the vehicles.

- The ground is assumed to be firm.
- The load distribution under the tracks is assumed to be concentrated under road wheels.
- The suspension springs are linear and identical.
- Unsuprung masses are neglected.
- The center of mass of the vehicles located in the geometrical center of the vehicles and all of the axles located symmetrically with respect to center of mass.
- First and last axle wheelbases and track widths are same for all of the vehicles.

3.3. Mathematical Modelling

The mathematical models of all the vehicles are same for general vehicle body dynamics. They differentiate in force generation between track and tire and steering angle between ASWV and SSWV. Firstly, general vehicle body dynamics equations will be given and after that force generation equations will be given.

3.3.1. Vehicle Body Dynamics

In this section, we consider two coordinate systems, one fixed to the ground *XYZ* which is the reference frame and one fixed to center of mass of the vehicles *xyz*. Initially these coordinate systems are coincident. The relation between the reference frame and body fixed vehicle frame will give the path taken by the vehicle in *XY* plane. One can see the relative position of the coordinate systems after movement of the vehicles in *Figure 13.*

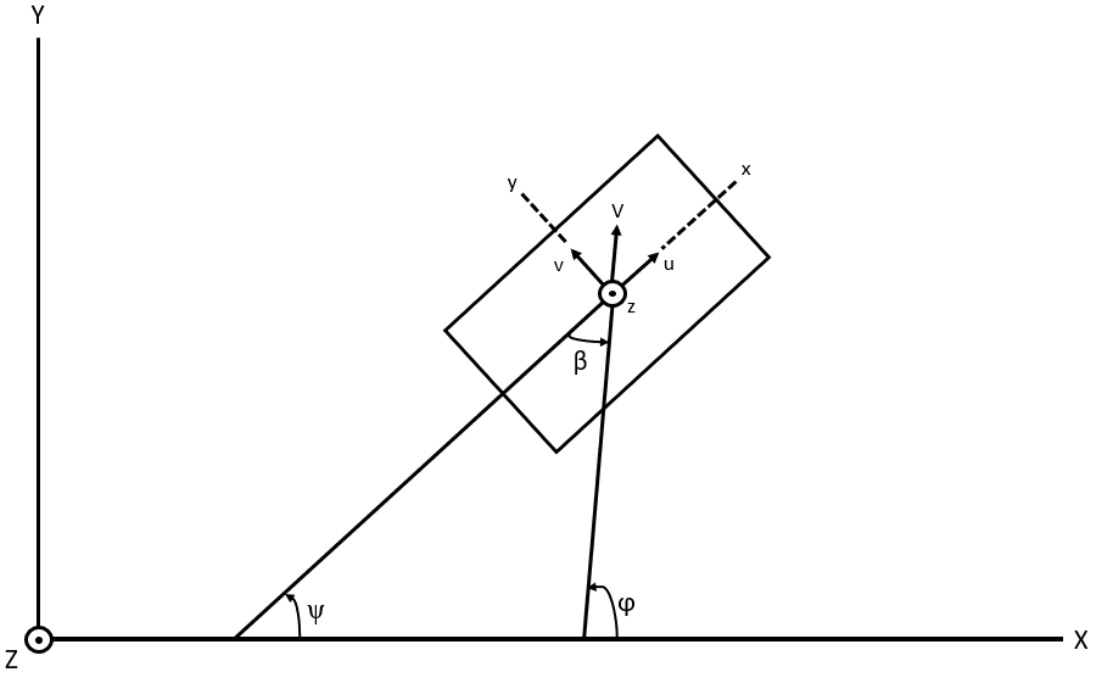

Figure 13. Coordinate systems, angles and velocities.

In *Figure 13, V* is the velocity vector of the vehicle; *u* is the *x*-axis component of the vehicle velocity in body fixed frame and *v* is the *y*-axis component of the vehicle velocity

in body fixed frame. ψ is the yaw angle, φ is the heading angle and β is the side slip angle. The heading angle φ is equal to $\psi + \beta$.

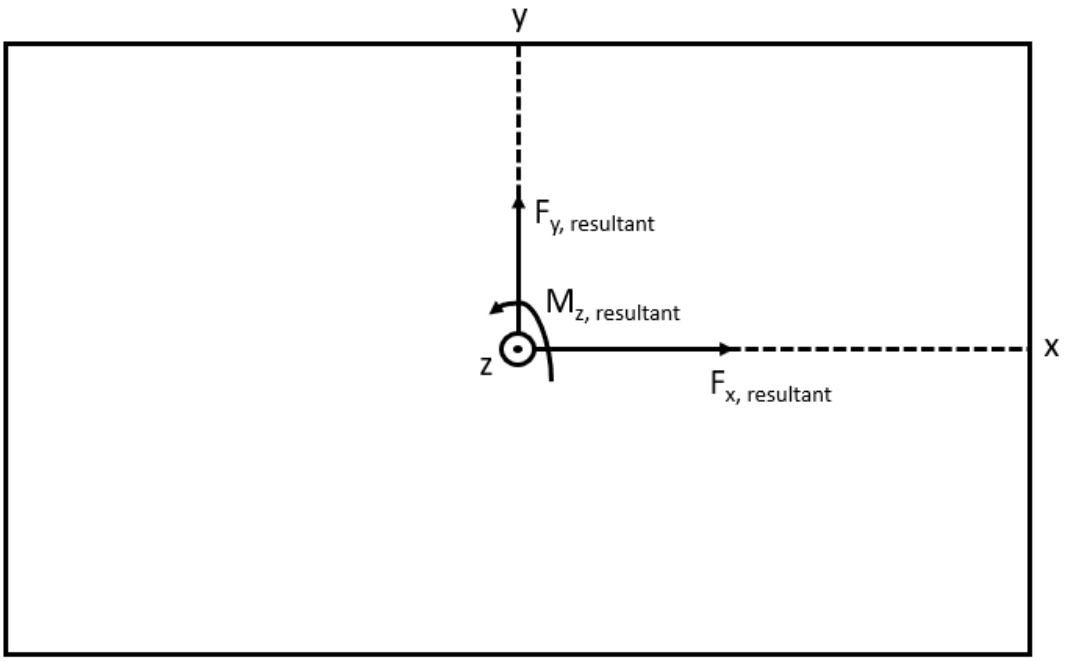

Figure 14. Resultant forces and moment acting on the center of mass.

The resultant forces and resultant moments about center of mass are shown in *Figure 14*. Three equation of motions can be written for 3 DOF planar motion of the vehicles.

$$ma_x = F_{x,\ resultant} \tag{3.1}$$

$$ma_y = F_{y,\ resultant} \tag{3.2}$$

$$I_z\ddot{\psi} = M_{z,\ resultant} \tag{3.3}$$

where m is the mass of the vehicle and I_z is the moment of inertia of the vehicle about the z axis in body fixed coordinate frame. r is the yaw rate and will be used instead of $\dot{\psi}$ from now on.

The Longitudinal and Lateral Accelerations

The longitudinal a_x and lateral a_y accelerations can be expressed as:

$$a_x = \dot{u} - vr \tag{3.4}$$

$$a_y = \dot{v} + ur \tag{3.5}$$

The derivation of Equation (3.4) and Equation (3.5) is given below [22]:

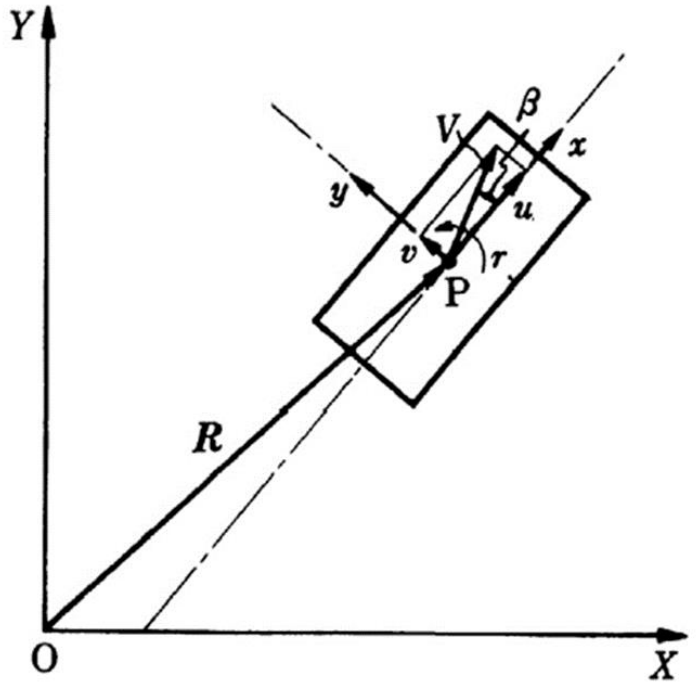

Figure 15 Coordinate axes for vehicle plane motion [22].

In *Figure 15*, $\boldsymbol{R}$ is the position vector, in the *X*-*Y* coordinate frame, of point P. The velocity vector $\dot{\boldsymbol{R}}$ and the acceleration vector $\ddot{\boldsymbol{R}}$ are:

$$\dot{\boldsymbol{R}} = u\boldsymbol{i} + v\boldsymbol{j} \tag{3.6}$$

$$\ddot{\boldsymbol{R}} = \dot{u}\boldsymbol{i} + u\dot{\boldsymbol{i}} + \dot{v}\boldsymbol{j} + v\dot{\boldsymbol{j}} \tag{3.7}$$

In *Figure 16*, the orientation between the unit vectors of ground fixed frame and the unit vectors of body fixed frame has been shown.

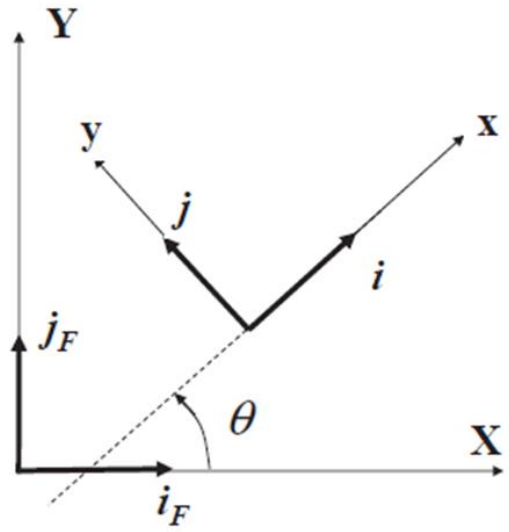

Figure 16 Unit vectors of ground fixed and body fixed coordinate frames [22].

The body fixed frame unit vectors can be written in terms of ground fixed unit vectors as follows:

$$\boldsymbol{i} = \cos\theta\, \boldsymbol{i}_F + \sin\theta\, \boldsymbol{j}_F \tag{3.8}$$

$$\boldsymbol{j} = -\sin\theta\, \boldsymbol{i}_F + \cos\theta\, \boldsymbol{j}_F \tag{3.9}$$

The derivatives of body fixed frame unit vectors:

$$\dot{\boldsymbol{i}} = -\dot{\theta}\sin\theta\, \boldsymbol{i}_F + \dot{\theta}\cos\theta\, \boldsymbol{j}_F = r(-\sin\theta\, \boldsymbol{i}_F + \cos\theta\, \boldsymbol{j}_F) = r\boldsymbol{j} \tag{3.10}$$

$$\dot{\boldsymbol{j}} = -\dot{\theta}\cos\theta\, \boldsymbol{i}_F - \dot{\theta}\sin\theta\, \boldsymbol{j}_F = -r(\cos\theta\, \boldsymbol{i}_F + \sin\theta\, \boldsymbol{j}_F) = -r\boldsymbol{i} \tag{3.11}$$

where $\boldsymbol{i}$ and $\boldsymbol{j}$ are the unit vectors of the body fixed coordinate frame whereas, $\boldsymbol{i}_F$ and $\boldsymbol{j}_F$ are the unit vectors of the ground fixed coordinate frame.

Substituting $\dot{\boldsymbol{i}}$ and $\dot{\boldsymbol{j}}$ into $\ddot{\boldsymbol{R}}$, we obtain:

$$\ddot{\boldsymbol{R}} = \underbrace{(\dot{u} - vr)\boldsymbol{i}}_{\boldsymbol{a_x}} + \underbrace{(\dot{v} + ur)\boldsymbol{j}}_{\boldsymbol{a_y}} \tag{3.12}$$

The resultant forces and resultant moments can be detailed as follows:

Longitudinal Forces

All of the longitudinal forces that are exerted on the vehicle can be written as:

$$F_{x,\ resultant} = F_{xL} + F_{xR} - F_{aero} - F_{incl} - F_{roll} \quad (3.13)$$

$$F_{xL} = \sum_{i=1}^{n} F_{xLi} \quad (3.14)$$

$$F_{xR} = \sum_{i=1}^{n} F_{xRi} \quad (3.15)$$

$$F_{aero} = \frac{1}{2} \rho\, A\, C_d V^2 \quad (3.16)$$

$$F_{incl} = m\, g \sin\theta \quad (3.17)$$

where F_{xLi} is the tractive force under i^{th} wheel for wheeled vehicles and road wheel for tracked vehicles and F_{xL} is the summation of all tractive forces in x direction at the left hand side of the wheel. F_{xR} and F_{xRi} are the right hand side forces and obey the description for left hand side above. F_{aero} is the aerodynamic force to which the vehicles are exposed from the front and ρ is the density of the air, A is the frontal area of the vehicle, C_d is the drag coefficient of the vehicle. F_{incl} is the weight component of the vehicle that is horizontal to inclination plane when a Θ degree of inclination exist and g is the acceleration of gravity. The longitudinal forces for a ten road wheel tracked vehicle can be seen in *Figure 19*.

Rolling Resistance of Vehicles

The rolling resistance of a wheeled vehicle can be calculated with the below formula for a wheeled vehicle [5]. Same formula can also be used for tracked vehicles.

$$F_{roll} = \sum_{i=1}^{n} F_{zLi}\left(f_r + k_r V\right) + \sum_{i=1}^{n} F_{zRi}\left(f_r + k_r V\right) \quad (3.18)$$

F_{roll} is the rolling resistance of the vehicles as seen in *Figure 17* and in *Figure 18*. F_{zLi} is the normal force wheel at the i^{th} axle and left side of the vehicle, while F_{zRi} represents the right side normal force. f_r and k_r are the rolling resistance coefficients of the wheels, V is the vehicle velocity.

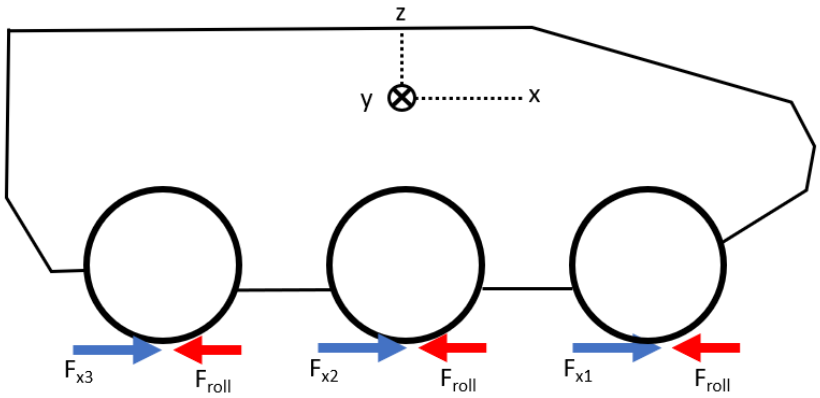

Figure 17 Rolling resistance force representation of a wheeled vehicle

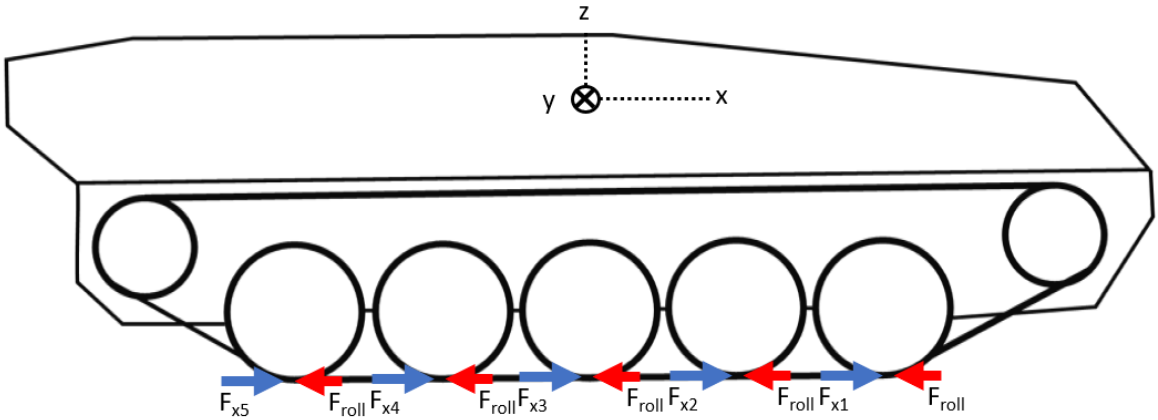

Figure 18 Rolling resistance force representation of a tracked vehicle

Lateral Forces

All of the lateral forces that are created under the vehicles can be summarized as:

$$F_{y,\ resultant} = F_{yL} + F_{yR} \tag{3.19}$$

$$F_{yL} = \sum_{i=1}^{n} F_{yLi} \tag{3.20}$$

$$F_{yR} = \sum_{i=1}^{n} F_{yRi} \tag{3.21}$$

where F_{yLi} is the y component of the tractive force under i^{th} wheel for wheeled vehicles and road wheel for tracked vehicles and F_{yL} is the summation of all tractive forces in y direction at the left side of the vehicle. F_{yR} and F_{yRi} are the right side forces. The lateral forces for a ten road wheel tracked vehicle can be seen in *Figure 19*.

Yaw Moments

The resultant moments about CG can be written as:

$$M_{z,\ resultant} = M_{FyL} + M_{FyR} + \left(F_{xR} - F_{xL}\right)\frac{t}{2} \tag{3.22}$$

$$M_{FyL} = \sum_{i=1}^{n} F_{yLi}\, x_i \tag{3.23}$$

$$M_{FyR} = \sum_{i=1}^{n} F_{yRi}\, x_i \tag{3.24}$$

where M_{FyL} and M_{FyR} are the moments about CG of the left and right track lateral forces respectively and t is the track width. A detailed representation of the forces that create moment on the CG for a ten road wheel tracked vehicle can be seen in *Figure 19*.

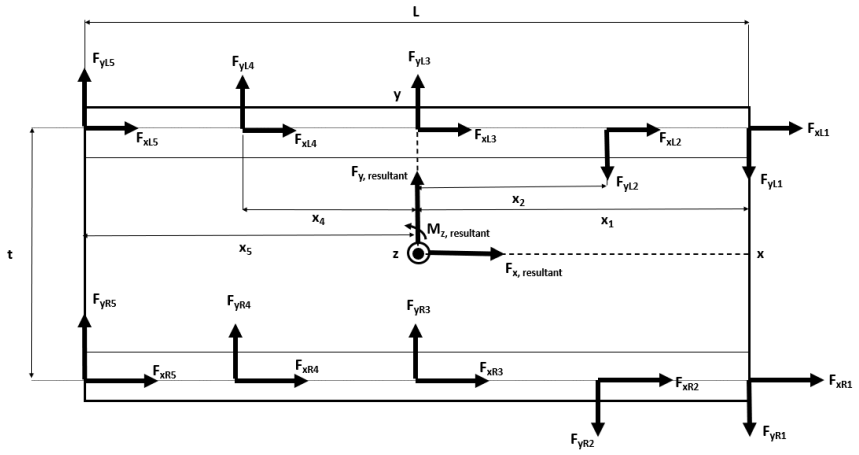

Figure 19 Resultant forces and moments on ten road wheel tracked vehicle.

Normal Forces

Normal forces on the wheels of wheeled vehicles and normal forces on the road wheels of the tracked vehicles can be expressed as follows [2]:

$$F_{zi} = F_{st,i} + \Delta F_{lon,i} + \Delta F_{lat,i} \tag{3.26}$$

where $F_{st,i}$, $\Delta F_{lon,i}$ and $\Delta F_{lat,i}$ are the statically distributed load, load transfer due to longitudinal acceleration and load transfer due to lateral acceleration respectively.

$$F_{st,i} = \frac{mg}{2}\left(\frac{\cos\theta}{n} - \frac{x_i}{\sum_{i=1}^{N} x_i^2} h_{cg} \sin\theta\right) \tag{3.27}$$

where n is the number of axles and h_{cg} is the height of the CG. x_i is the distance between the i^{th} axle and CG in x direction. x_i is positive when the axle is in front of the CG and is negative when the axle is behind of the CG.

$$\Delta F_{lat,i} = \pm \frac{m a_y h_{cg}}{tn} \tag{3.28}$$

where a_y is the lateral acceleration of the vehicle and + sign is valid for right side of the vehicle whereas – sign is valid for left side of the vehicle.

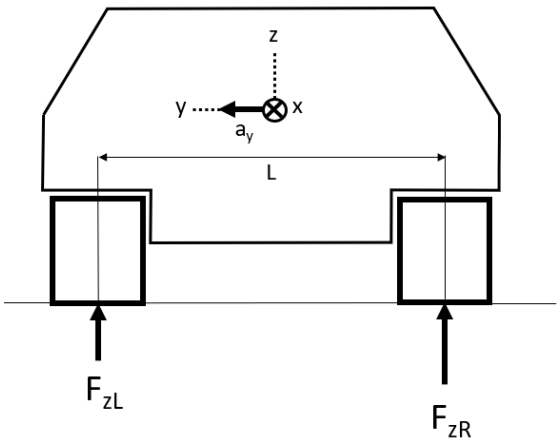

Figure 20 Lateral load transfer between right and left side of the vehicle.

$$\Delta F_{long,i} = k_i \Delta z_i \tag{3.29}$$

Due to the pitch motion longitudinal weight transfer exists. To calculate the longitudinal load transfer, a statically indeterminate situation has to be solved, since the number of the axles are more than two. To solve a statically indeterminate problem the stiffnesses of the suspensions has to be included. In the above Equation (3.7) k_i is the vertical stiffness and Δz_i is the relative displacement between road wheel and vehicle body due to pitch motion only. In reality Δz_i occurs due to both pitch and roll motions of the vehicle body. But, here only the portion that is occurred because of the pitch motion of the body, has been considered. As a matter of fact, pitch motion affects longitudinal weight transfer whereas roll motion affects lateral load transfer which has already been calculated before.

Δz_i for each axle can be calculated by the following expression:

$$\Delta z_i = x_i \tan\gamma \tag{3.30}$$

where γ is the pitch angle of the vehicle body. The pitch angle γ can be calculated by forming a moment balance equation about point *O* on the ground, as seen in *Figure 21*.

$$(F_{aero} + ma_x)h_{cg} + K_p\gamma = 0 \tag{3.31}$$

where K_p is the pitch stiffness of the vehicle body. Alternatively, this moment balance can be expressed as follows:

$$(F_{aero} + ma_x)h_{cg} + \sum_{i=1}^{n}(F_{zi})x_i = 0 \tag{3.32}$$

This moment balance is not a dynamic equation, it is a static equation. In the scope of this thesis, the tracks and tires are working only in traction mode. The braking movements have not been modelled. So, there is no sudden change in longitudinal acceleration accounting the vehicle sizes (the assumed vehicle mass is 30 tons). Based on this

information, the derivative of the pitch angle can be neglected. But in the simulation, the aerodynamic force F_{aero} and longitudinal acceleration a_x are being calculated in every loop. Therefore, the pitch angle is calculated incrementally in every loop.

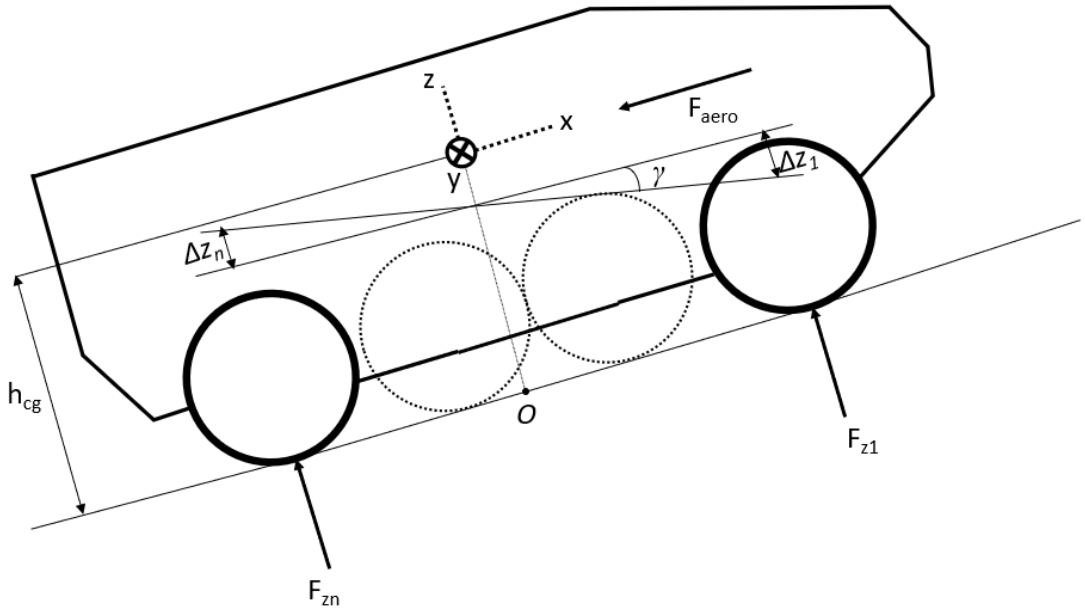

Figure 21. Resultant forces and moment acting on the center of mass.

The normal forces that appear in the Equation (3.10) can be reduced to only longitudinal weight transfers since all the other forces will cancel each other out while taking moment balance about CG:

$$\sum_{i=1}^{n}(F_{zi})x_i = \sum_{i=1}^{n}(\Delta F_{long,i})x_i \tag{3.33}$$

By substituting 3.7 and 3.8 into 3.10 and equating to 3.9 K_p can be found as:

$$K_p = \sum_{i=1}^{n} k_i x_i^2 \tag{3.34}$$

With K_p found, $\Delta F_{lon,I}$ can be calculated.

Rigid Body Kinematics

To calculate each velocity component under each road wheel below kinematic calculations have been carried out.

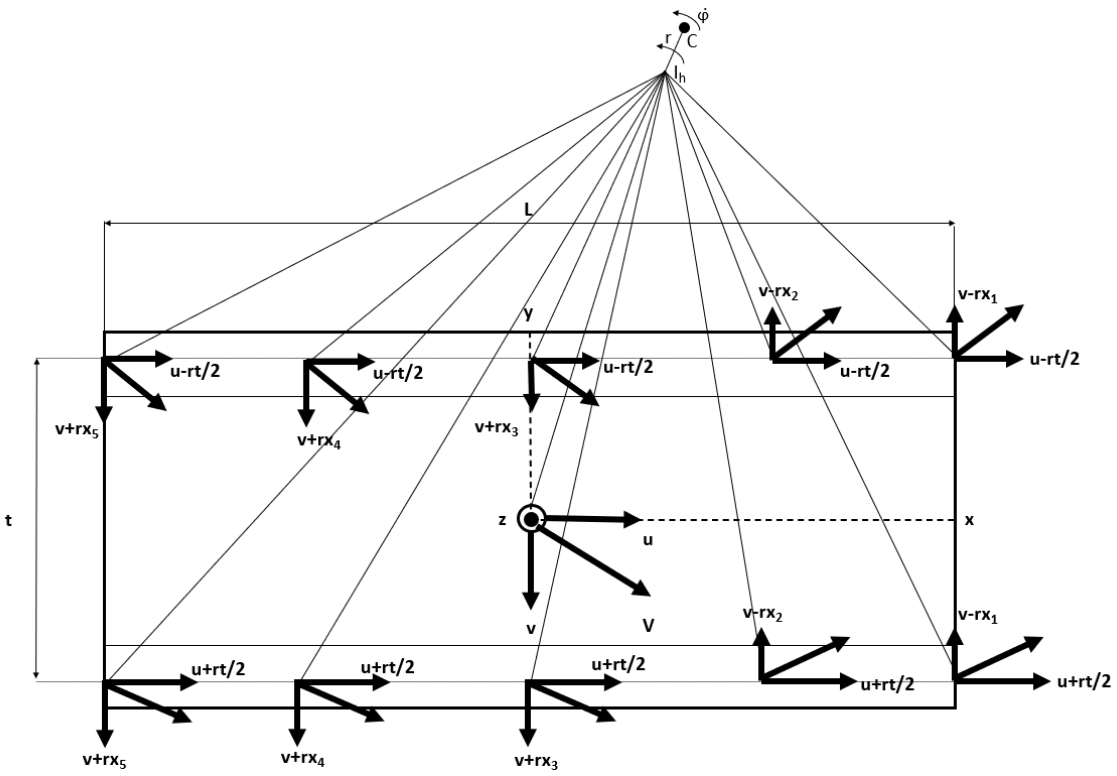

Figure 22. Kinematics of the vehicle body.

In *Figure 22* the rigid body kinematics of the vehicle have been represented. *t* is the track width and *L* is the wheelbase. The CG is located in the middle of the vehicle. For all of the vehicles below relation holds:

$$x_1 = x_n = \frac{L}{2} \tag{3.35}$$

Independent from the number of axles all of the remaining axles are located between last and first axle with equal space.

When the vehicle is undergoing a maneuver, due to rigid body assumption, different points of the vehicle possess different velocities with respect to CG. Below expressions are the velocity components of the points on the vehicle body above road wheels for tracked vehicles or above wheels for wheeled vehicles in *xyz* frame:

$$u_{Li} = u - r\frac{t}{2} \tag{3.36}$$

$$u_{Ri} = u + r\frac{t}{2} \tag{3.37}$$

$$v_{Li} = v + r\,x_i \tag{3.38}$$

$$v_{Ri} = v_{Li} \tag{3.39}$$

where x_i are positive when the axle is in front of the CG and are negative when the axle is behind of the CG.

Vehicle Trajectory and Turn Radius

To find the trajectory of the vehicles, translation between body fixed frame and ground fixed frame is needed.

The *X* and *Y* components of the velocity in ground fixed *XYZ* frame is as follows:

$$\dot{X} = u\cos\psi - v\sin\psi \tag{3.40}$$

$$\dot{Y} = u\sin\psi + v\cos\psi \tag{3.41}$$

Location and orientation of the vehicle in ground fixed *XYZ* coordinate system can be designated by following expressions:

$$X = \int_0^t \dot{X}\, dt \tag{3.42}$$

$$Y = \int_0^t \dot{Y}\, dt \tag{3.43}$$

$$\psi = \int_0^t r\, dt \tag{3.44}$$

Radius of curvature, as stated in [14], can be calculated by:

$$R_c = \frac{V}{r} \tag{3.45}$$

3.3.2. Force Generation

There are two main types of vehicles in the scope of this thesis, wheeled and tracked. They differentiate in force generation mechanisms. Wheeled vehicles generate traction forces via tires when slip occurs. Ackermann steering adds another level of difference to the force generation mechanism. Tracked vehicles generate traction forces majorly from the track pads that are right under the road wheels when slip occurs.

3.3.2.1. Wheeled Vehicle Force Generation

Tire ground relations are mostly modelled with Magic Formula [12] or Dugoff Tire Model [11]. But here the main goal is to compare tracked vehicle and wheeled vehicle maneuvering performances, so it has been needed to use same traction force generation theory for both wheeled and tracked vehicles. The flexible pad theory [1] has been used for both types of the vehicles.

For the left hand side tires the traction forces are:

$$F_{xLi} = \left(\frac{s_{Li}}{(s_{Li}^2+tan^2\alpha_{Li})^{0.5}}\right) 0.94\, \mu\, F_{zLi} \left(1 - e^{-10.7(s_{Li}^2+tan^2\alpha_{Li})^{0.5}}\right) \tag{3.46}$$

$$F_{yLi} = \left(\frac{\tan\alpha_{Li}}{(s_{Li}^2+tan^2\alpha_{Li})^{0.5}}\right) 0.94\, \mu\, F_{zLi} \left(1 - e^{-10.7(s_{Li}^2+tan^2\alpha_{Li})^{0.5}}\right) \tag{3.47}$$

For the right hand side tires the traction forces are:

$$F_{xRi} = \left(\frac{s_{Ri}}{(s_{Ri}^2+tan^2\alpha_{Ri})^{0.5}}\right) 0.94\ \mu\ F_{zRi}\left(1 - e^{-10.7(s_{Ri}^2+tan^2\alpha_{Ri})^{0.5}}\right) \quad (3.48)$$

$$F_{yRi} = \left(\frac{tan\ \alpha_{Ri}}{(s_{Ri}^2+tan^2\alpha_{Ri})^{0.5}}\right) 0.94\ \mu\ F_{zRi}\left(1 - e^{-10.7(s_{Ri}^2+tan^2\alpha_{Ri})^{0.5}}\right) \quad (3.49)$$

where s_{Li} and α_{Li} are longitudinal slips and slip angles of the i^{th} axle at the left hand side of the vehicle respectively. s_{Ri} and α_{Ri} are longitudinal slips and slip angles of the i^{th} axle at the right hand side of the vehicle respectively. μ is the friction coefficient and δ_{Li} is the steering angle of the wheel on the i^{th} axle and left hand side of the vehicle.

$$s_{Li} = \frac{r_w\omega_{Li} - u_L}{r_w\omega_{Li}} \quad (3.50)$$

$$\alpha_{Li} = atan\left(\frac{v_{Li}}{u_L}\right) - \delta_{Li} \quad (3.51)$$

Same slip equations hold for the right side of the vehicle.

$$s_{Ri} = \frac{r_w\omega_{Ri} - u_R}{r_w\omega_{Ri}} \quad (3.52)$$

$$\alpha_{Ri} = atan\left(\frac{v_{Ri}}{u_R}\right) - \delta_{Ri} \quad (3.53)$$

For skid steering wheeled vehicle the steering angles of the wheels are simply zero.

3.3.2.2. Tracked Vehicle Force Generation

As mentioned in the previous section the flexible pad theory [1] has been used also for the tracked vehicles. The traction equations for tracked vehicles for the left hand side are:

$$F_{xLi} = \left(\frac{s_L}{(s_L^2+tan^2\alpha_{Li})^{0.5}}\right) 0.94\ \mu\ F_{zLi}\left(1 - e^{-10.7(s_L^2+tan^2\alpha_{Li})^{0.5}}\right) \quad (3.54)$$

$$F_{yLi} = \left(\frac{\tan\alpha_{Li}}{(s_L^2+tan^2\alpha_{Li})^{0.5}}\right) 0.94\ \mu\ F_{zLi}\left(1 - e^{-10.7(s_L^2+tan^2\alpha_{Li})^{0.5}}\right) \quad (3.55)$$

For the right hand side tires the traction forces are:

$$F_{xRi} = \left(\frac{s_R}{(s_R^2+tan^2\alpha_{Ri})^{0.5}}\right) 0.94\ \mu\ F_{zRi}\left(1 - e^{-10.7(s_R^2+tan^2\alpha_{Ri})^{0.5}}\right) \quad (3.56)$$

$$F_{yRi} = \left(\frac{tan\ \alpha_{Ri}}{(s_R^2+tan^2\alpha_{Ri})^{0.5}}\right) 0.94\ \mu\ F_{zRi}\left(1 - e^{-10.7(s_R^2+tan^2\alpha_{Ri})^{0.5}}\right) \quad (3.57)$$

It can be easily seen that the longitudinal slip values for tracked vehicles do not change from axle to axle. All of the longitudinal slips are the same for the road wheels on the same track.

$$s_L = \frac{V_{tL}-u_L}{V_{tL}} \quad (3.58)$$

$$\alpha_{Li} = atan\left(\frac{v_{Li}}{u_L}\right) \quad (3.59)$$

Same slip equations hold for the right side of the vehicle.

$$s_R = \frac{V_{tR}-u_R}{V_{tR}} \quad (3.60)$$

$$\alpha_{Ri} = atan\left(\frac{v_{Ri}}{u_R}\right) \quad (3.61)$$

where V_{tL} and V_{tR} are the left and right track speeds respectively.

3.5 Stability Analysis

The understeer gradients of wheeled vehicles have been studied thoroughly in the literature. Understeer, neutral steer and oversteer definitions and their effects on the

vehicle performance have been represented widely in the literature for wheeled vehicles. Bayar [5] has derived stability equations for three and four axle wheeled and Ackermann steered vehicles. In these derivations the characteristic equations of the systems have been found and necessary and sufficient conditions for stability criteria have been designated as follows:

For three axle vehicle, the following relations hold:

1) Neutral steer for $aC_f = bC_m + cC_r$
2) Understeer for $aC_f > bC_m + cC_r$ or $|aC_f| < |bC_m + cC_r|$
3) Oversteer for $aC_f < bC_m + cC_r$ or $|aC_f| > |bC_m + cC_r|$

where *a*, *b* and *c* are the distance between first, second and third axle and CG respectively. C_f, C_m and C_r are the cornering stiffnesses of the first, second and third axles respectively.

For four axle vehicle, the following relations hold

1) Neutral steer for $aC_1 + bC_2 = cC_3 + dC_4$
2) Understeer for $aC_1 + bC_2 > cC_3 + dC_4$ or $|aC_1 + bC_2| < |cC_3 + dC_4|$
3) Oversteer for $aC_1 + bC_2 < cC_3 + dC_4$ or $|aC_1 + bC_2| > |cC_3 + dC_4|$

where *d* is the distance between fourth axle and CG and C_1, C_2, C_3 and C_4 are the first, second, third and fourth axle cornering stiffnesses respectively.

Ni, Hu and Li [6] have defined stability factors for four axle skid steered and four axle Ackermann steered vehicles:

$$K_{skid} = \frac{2m(cK_{y3}+dK_{y4}-aK_{y1}-bK_{y2})}{4A+B^2(K_{x1}+K_{x2}+K_{x3}+K_{x4})(K_{y1}+K_{y2}+K_{y3}+K_{y4})} \quad (3.62)$$

$$K_{Ackermann} = \frac{m(cK_{y3}+dK_{y4}-aK_{y1}-bK_{y2})}{2A} \quad (3.39)$$

where *A*:

$$A = (a+c)^2K_{y1}K_{y3} + (a+d)^2K_{y1}K_{y4} + (b+c)^2K_{y2}K_{y3} + (b+d)^2K_{y2}K_{y4} \quad (3.63)$$

K_{y1}, K_{y2}, K_{y3} and K_{y4} are cornering stiffnesses and K_{x1}, K_{x2}, K_{x3} and K_{x4} are longitudinal stiffnesses. The vehicle has been set as understeer if $K>0$, neutral steer if $K=0$ and oversteer if $K<0$.

As can be seen from both above approaches the deciding factor for vehicle handling characteristics is the sign of the numerator part of the stability factor or understeer gradient. For the scope of this thesis, the sign of the stability factor or understeer gradient is fair enough to proceed. For both wheeled and six road wheel tracked vehicles Bayar's stability definition for a three axle vehicle will be adequate and for eight road wheel tracked vehicle Bayar's stability definition for a four axle vehicle will be adequate. So, it has been assumed to be valid if below definitions have been made for ten road wheel tracked vehicle:

1) Neutral steer for $aC_1 + bC_2 = dC_4 + eC_5$
2) Understeer for $aC_1 + bC_2 > dC_4 + eC_5$ or $|aC_1 + bC_2| < |dC_4 + eC_5|$
3) Oversteer for $aC_1 + bC_2 < dC_4 + eC_5$ or $|aC_1 + bC_2| > |dC_4 + eC_5|$

where *e* is the distance between fifth axle and CG, C_5 is the fifth axle cornering stiffness. The traction force generation has been explained in the previous section. The flexible pad formula has been applied for tracked vehicles and it has been adapted to wheeled vehicles. The cornering stiffness is the generated force for per slip angle. In static conditions, all the cornering stiffnesses of the tires and of the track pads under the road wheels are same. Therefore, all vehicles appear to be neutral steer in linear conditions since the CG is located at the center of the vehicle. But, the traction force generation method in this thesis cannot be simplified to find a cornering stiffness for the purpose of determining vehicle

handling characteristics. Under combined slip and normal force changes on the wheels, caused by roll and pitch body motions, generated lateral force for an arbitrary slip angle changes with respect to driving conditions. So, the vehicle responses in the simulation scenarios will reveal the non-linear behavior and the handling characteristics of the vehicles.

Similar non-linear handling behavior can be seen in the literature. Below graph represents the change in the stability characteristics of an Ackermann steered passenger vehicle under high lateral accelerations [14].

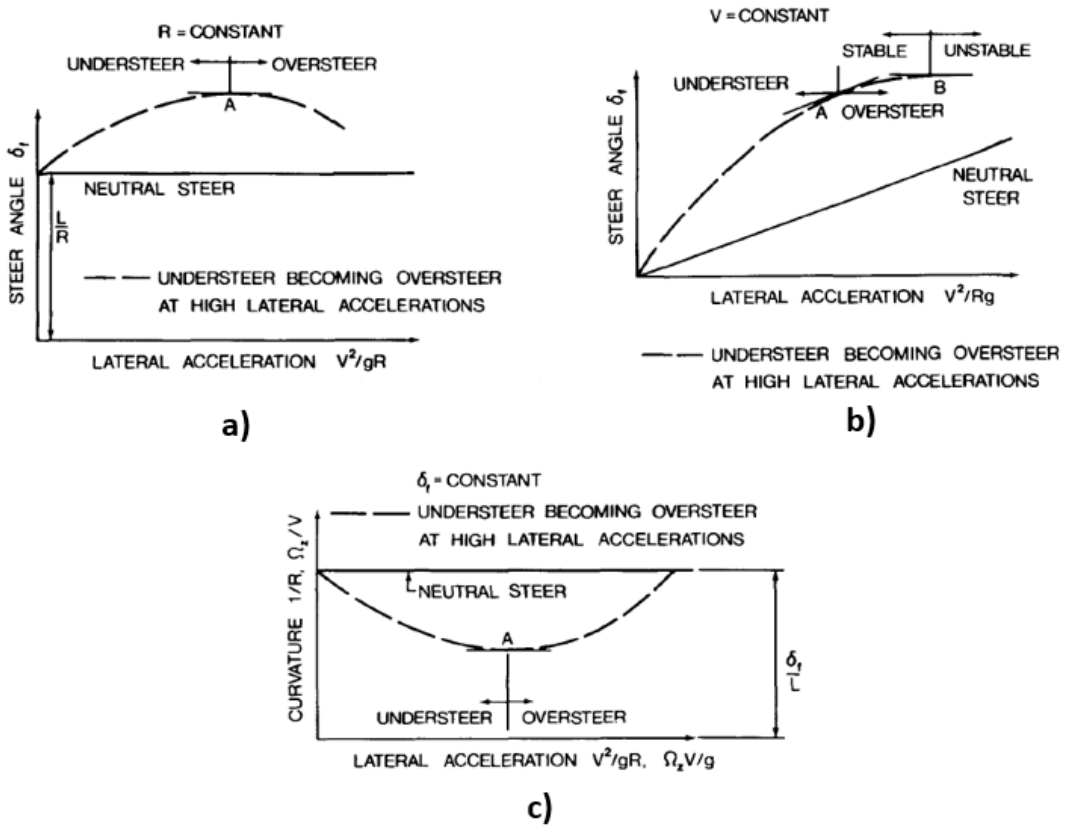

Figure 23. a) Constant radius, b) Constant Speed, c) Constant Steering angle [14]

4. SIMULATION RESULTS

4.1 Introduction

The modelled vehicles have been subjected to various simulation scenarios to understand the nature and difference of their behaviors. There are two inputs to the vehicle models, which are wheel or track speed and steering angle or speed difference between left and right side of the vehicle. These inputs have been manipulated to test the models and to reach the desired maneuvers.

At first, the skid steering capable vehicles have been made to execute point turn maneuvers. These vehicles are skid steering wheeled vehicle and tracked vehicles. Secondly, constant radius turns with varying speeds have been investigated. All of the vehicles executed 15 m, 100 m and 1000 m radius turns.

To analyze the steady state behavior of the vehicles yaw rate gain and radius gain curves have been gathered for same steering input and varying speeds. Also, the reasons behind the vehicle behaviors have been investigated with some literature studies and parameter changes in this model. Another analysis has been carried out for left and right sprocket torques and lateral coefficient of friction values at different speeds and varying turn radii.

4.2 Point Turn Maneuvers

All of the skid steering vehicles have ability to execute point turn maneuver. To make a point turn maneuver same track or wheel speeds must be applied to left and right sides in opposite directions. The applied speeds can be seen in . A zero radius has been expected for this maneuver with zero longitudinal and lateral speeds. Below graph *Figure 24*

belongs to six road wheel tracked vehicle and shows resulting speeds, slips and tractions forces.

Table 2 Speed inputs to skid steering vehicles to execute point turn maneuvers

Vehicle Type	Track or Wheel Speed
Skid Steered Wheeled Vehicle	3 m/s
	7 m/s
	10 m/s
Six Road Wheel Tracked Vehicle	3 m/s
	7 m/s
	10 m/s
Eight Road Wheel Tracked Vehicle	3 m/s
	7 m/s
	10 m/s
Ten Road Wheel Tracked Vehicle	3 m/s
	7 m/s
	10 m/s

Modelling a point turn maneuver for skid steering vehicles requires a delicate attention. Left and right hand side tracks or wheels are turning in opposite directions at the same speed. The slip calculation method bears an important role. It has to be capable of calculating all of the vehicle movements with right sign. For a point turn maneuver the longitudinal slips, that are created at the left and right sides of the vehicle, have opposite signs but, they are same in magnitude. On the other hand, the slip angles, that are in front of the CG and behind of the CG, have opposite signs but, symmetric points with respect to CG are same in magnitude.

During a point turn maneuver some of the vehicle body movements are expected to be resulted as zero such as, vehicle longitudinal velocity, vehicle lateral velocity etc. These variables may be in the denominator parts in some of the equations. These calculations require an important attention. When denominator is zero the result may be infinite or

may be uncertain. Adequate precautions need to be taken, such as usage of if/ else conditions in order to proceed without any error.

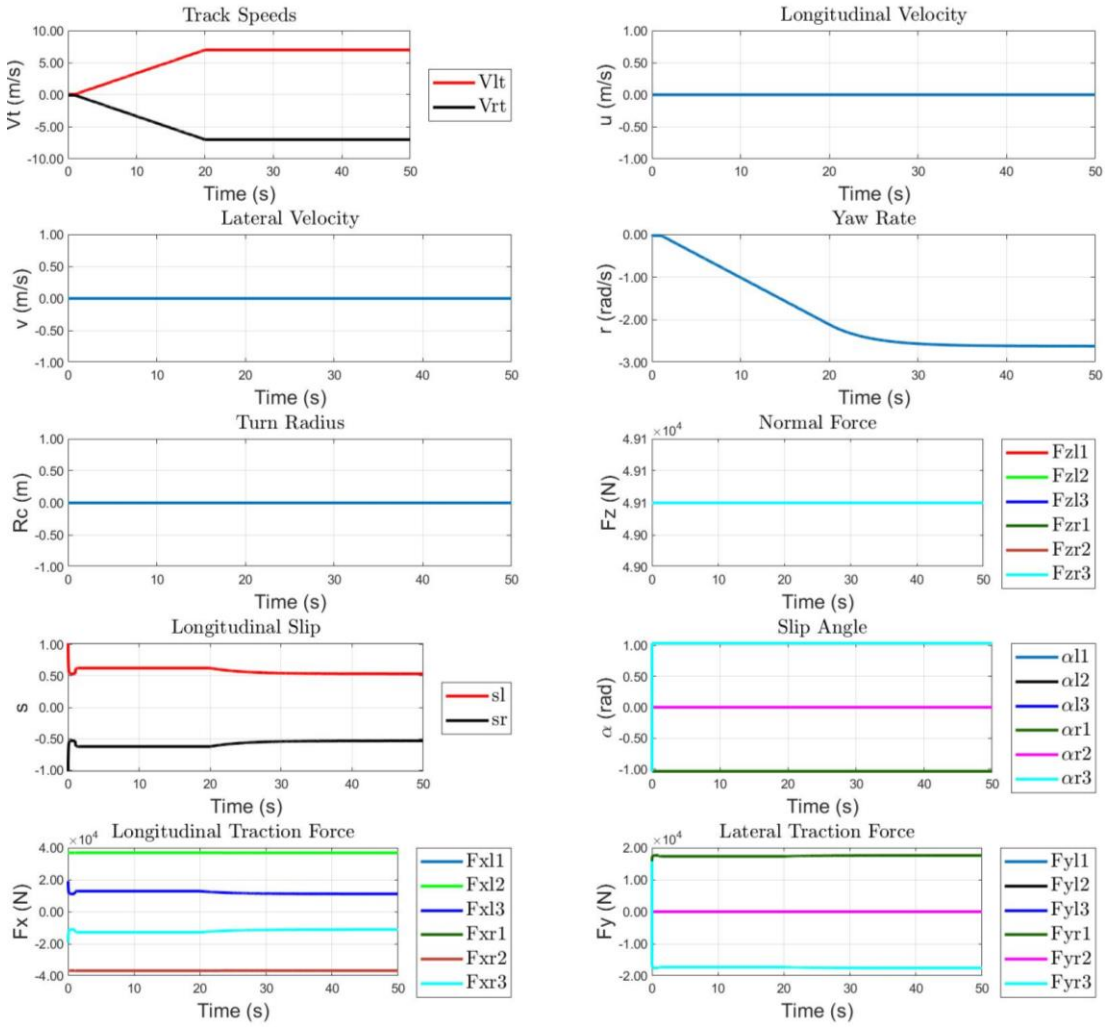

Figure 24. Point turn of six road wheeled tracked vehicle at 7 m/s track speed input.

The longitudinal and lateral velocities and turn radius are resulted zero as expected. Normal force distributions are same for all wheels since there is no pitch and roll motions as the CG is geometrically symmetric.

4.3 Constant Radius Turns

All of the vehicles have been subjected to constant radius turn maneuvers for 15 m, 100 m and 1000 m radii at 3 m/s, 7 m/s and 10 m/s vehicle speeds as seen in .

Table 3 Speed inputs to all vehicles to execute constant radius turn maneuvers

Vehicle Type	Turn Radius / Track or Wheel Speed	15 m turn radius	100 m turn radius	1000 m turn radius
Ackermann Steered Wheeled Vehicle	3 m/s	✔	✔	✔
	7 m/s			
	10 m/s			
Skid Steered Wheeled Vehicle	3 m/s	✔	✔	✔
	7 m/s			
	10 m/s			
Six Road Wheel Tracked Vehicle	3 m/s	✔	✔	✔
	7 m/s			
	10 m/s			
Eight Road Wheel Tracked Vehicle	3 m/s	✔	✔	✔
	7 m/s			
	10 m/s			
Ten Road Wheel Tracked Vehicle	3 m/s	✔	✔	✔
	7 m/s			
	10 m/s			

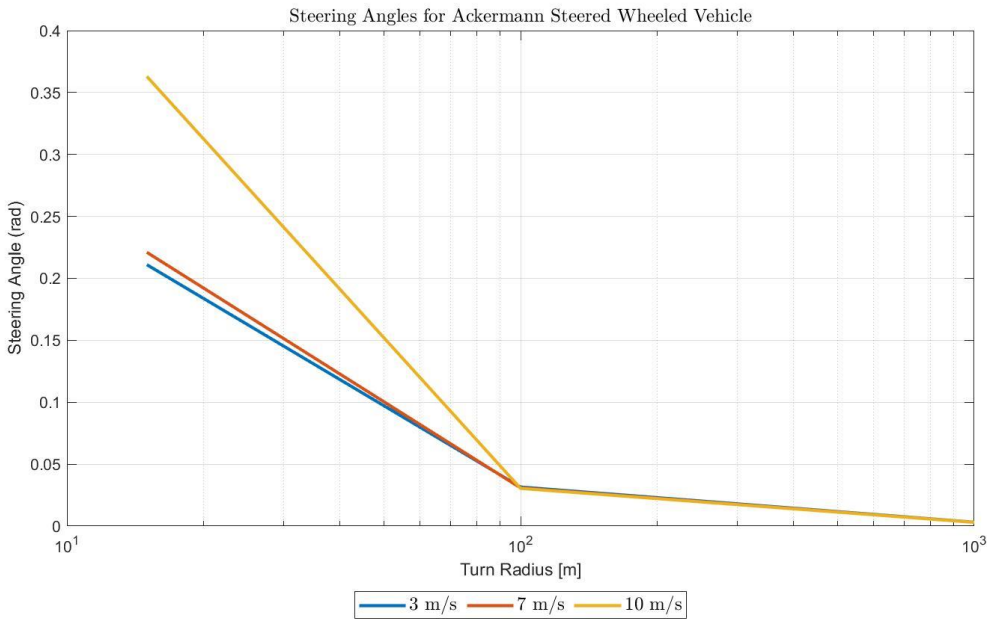

Figure 25. Required steering angles of Ackermann steered wheeled vehicle for constant radius turns at different speeds.

In *Figure 25*, the steering angle have to be increased to make same radius at higher speeds, which indicates the Ackermann steered vehicle shows understeer behavior.

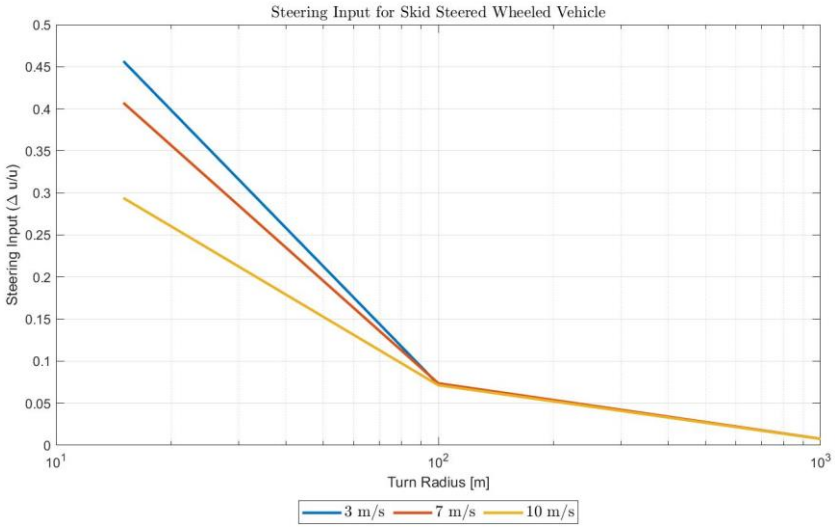

Figure 26. Required steering input of skid steered wheeled vehicle for constant radius turns at different speeds.

Contrary to Ackermann steered wheeled vehicle, skid steered wheeled vehicle shows oversteering behaviors since required steering input decreases as the speed of the vehicle increases, as seen in *Figure 26*.

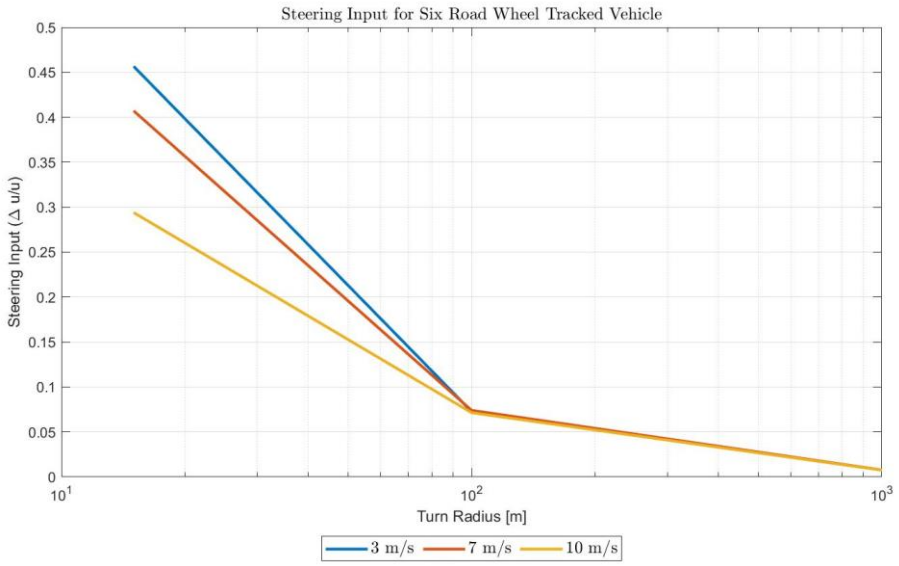

Figure 27. Required steering input of six road wheel tracked vehicle for constant radius turns at different speeds.

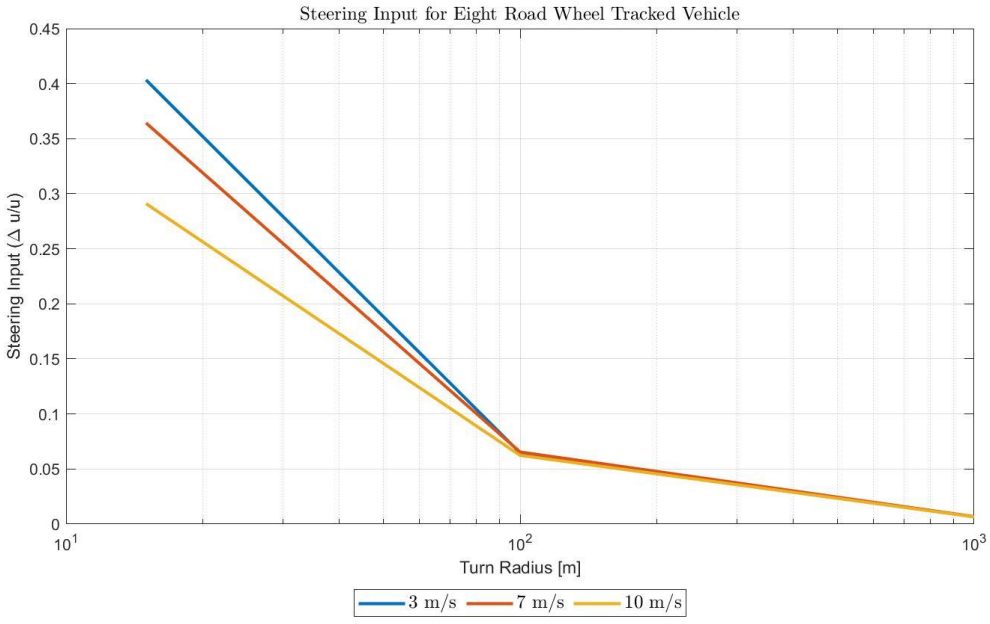

Figure 28. Required steering input of eight road wheel tracked vehicle for constant radius turns at different speeds.

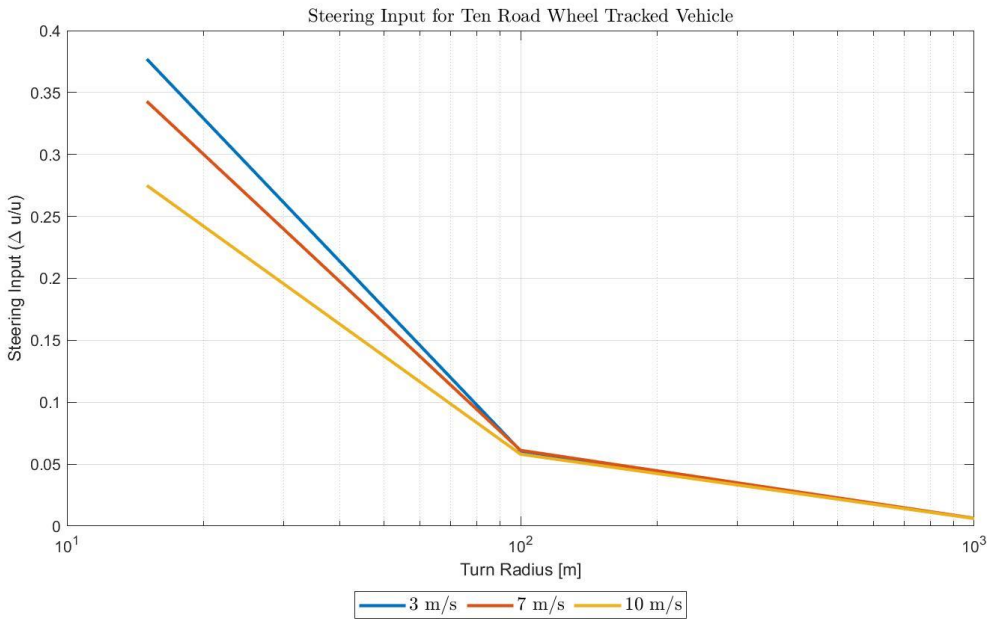

Figure 29. Required steering input of ten road wheel tracked vehicle for constant radius turns at different speeds.

The track vehicles show oversteering behaviors as the need for steering input to keep the same radius of turn decreases with increasing speeds. As seen in *Figure 27*, *Figure 28* and *Figure 29*.

To compare the vehicles with each other, below graphs needed.

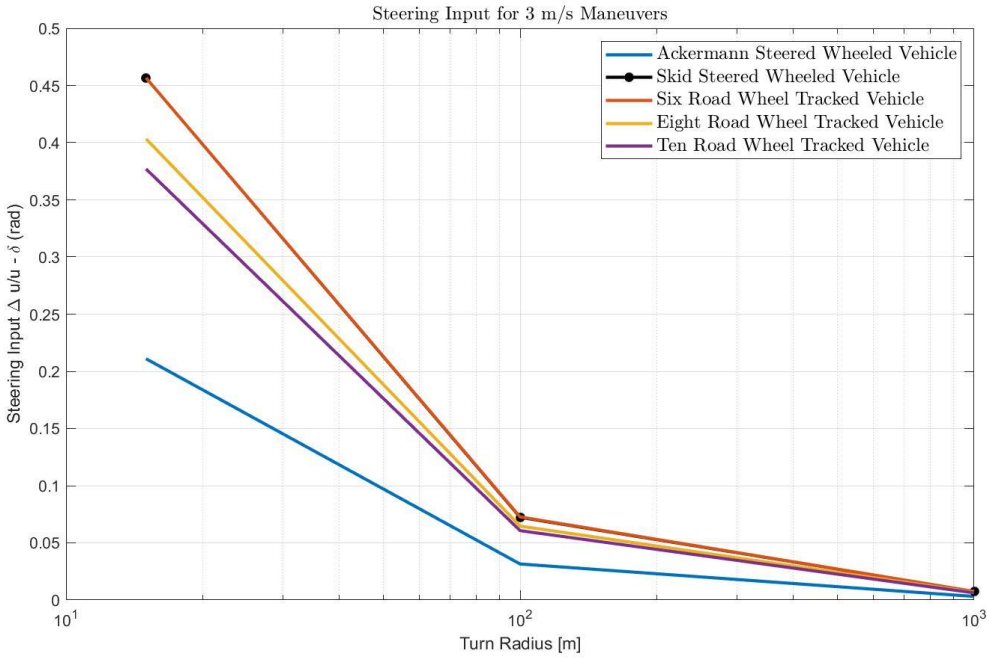

Figure 30. Required steering angles of all vehicles for constant radius turns at 3 m/s speed.

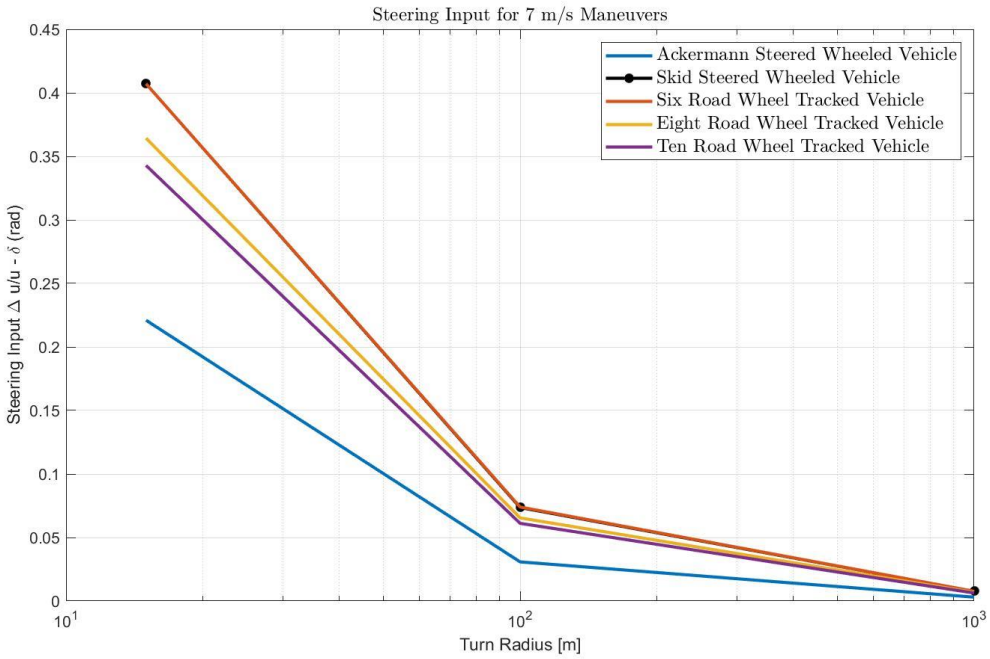

Figure 31. Required steering angles of all vehicles for constant radius turns at 7 m/s speed.

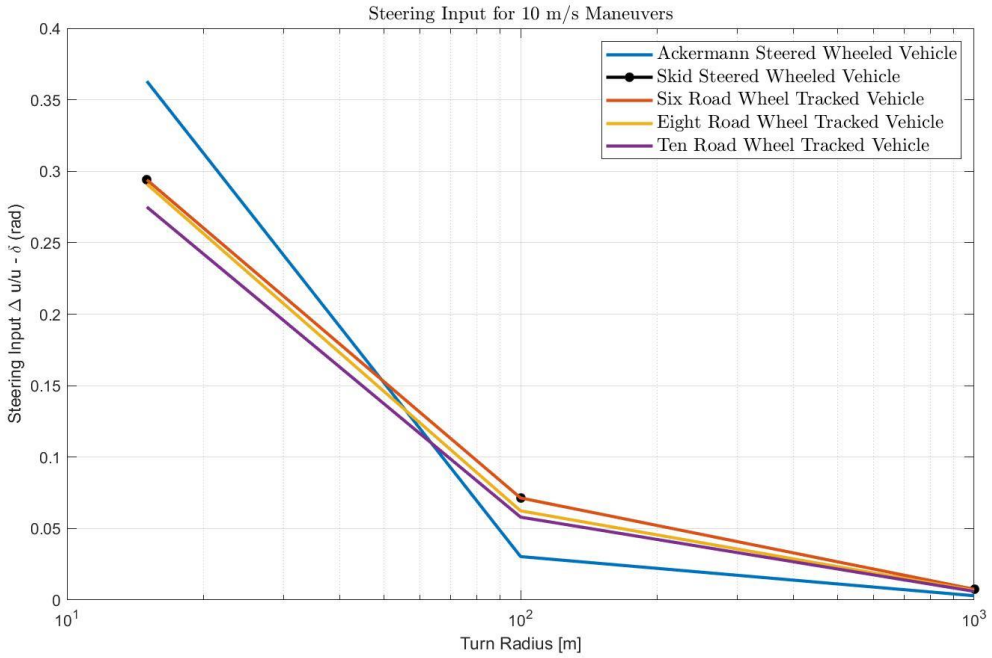

Figure 32. Required steering angles of all vehicles for constant radius turns at 10 m/s speed.

The Ackermann steered vehicle behaves differently than skid steering vehicles since a steering angle exists. The steering input to skid steering vehicle is $\frac{\Delta u}{u}$ where Δu is the speed difference between left and right tracks for tracked vehicles or wheels for the skid steered wheeled vehicles. So, it cannot be directly compared with the skid steered vehicles. But a legitimate command can be made from the trend of the behaviors.

From above *Figure 30*, *Figure 31* and *Figure 32* it can be seen that for the same radius of turn at the same speed skid steered wheeled vehicle always requires same amount of steering input as six road wheel tracked vehicle. Since all the dynamics equations were the same and same traction generation theory has been used this outcome was expected.

Between the tracked vehicles the ten road wheeled tracked vehicle always requires smaller amount of steering input. Whereas eight road wheeled tracked vehicle requires steering input larger than the ten road wheel tracked vehicle and smaller than the six road wheel tracked vehicle. So, there is a direct relation between the number of road wheels and required steering input. As the number road wheels increases the load of the vehicle distributed more and agility of the vehicle increases.

Below graphs show yaw rate responses of the all vehicles. Since the radius of turns and the speed that the path taken are the same yaw rates of all vehicles are similar. As can be seen from *Figure 33- Figure 34.*

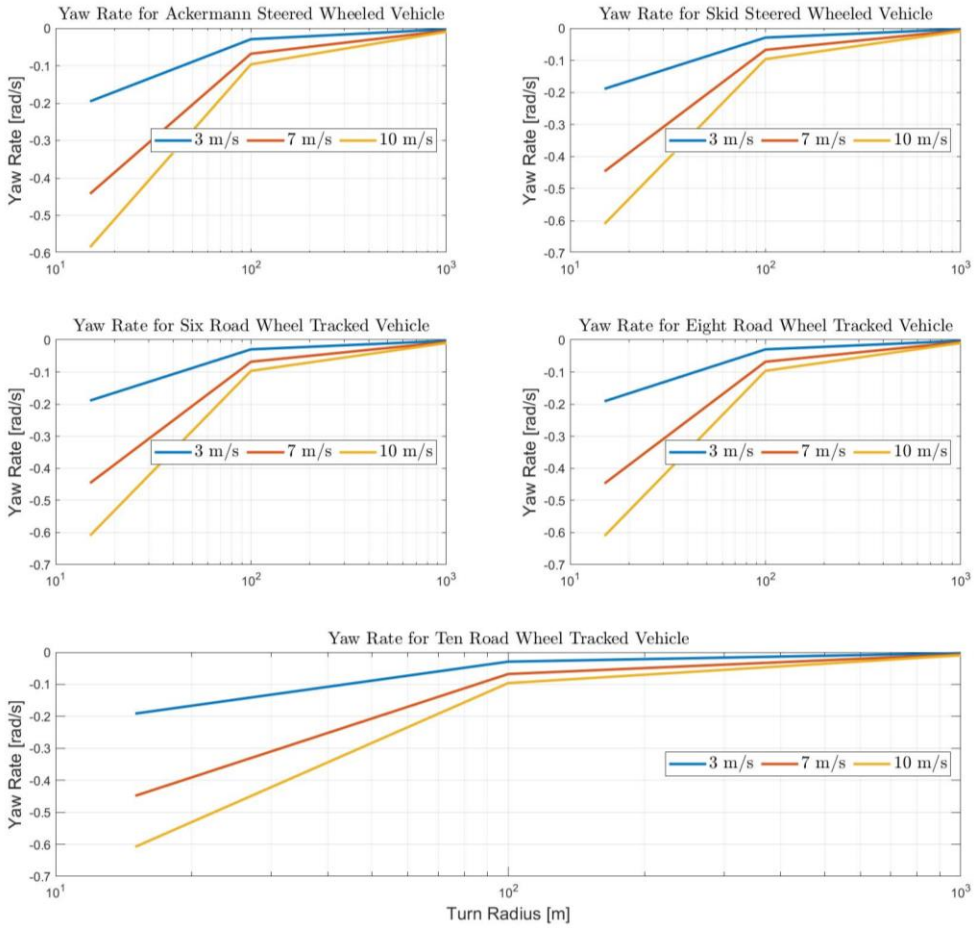

Figure 33 Yaw Rate of all vehicles at different vehicle speeds for constant turn radii

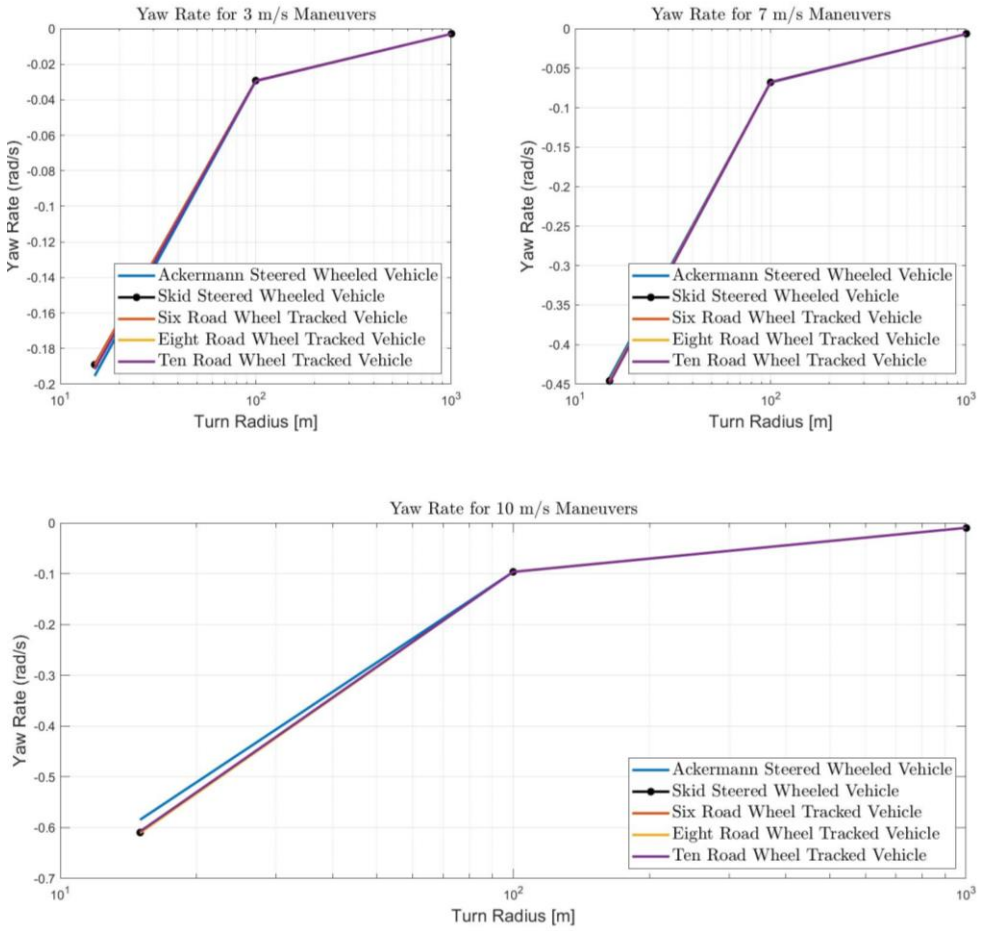

Figure 34 Yaw Rate of all vehicles at the same speed for constant turn radii

For the sake of clarity, some outputs of the constant turn maneuvers are represented below. The constant turn maneuvers are composed of three different turn radii, three different vehicle speeds for five types of the vehicles, this sums up to 45 different simulations. A sample of five simulations has been given for 100 m radius at 7 m/s for all the vehicles. Lateral, longitudinal velocities, yaw rates and turn radii with the taken path, lateral, longitudinal slips and forces with normal force distributions are given in *Figure 35-Figure 44*.

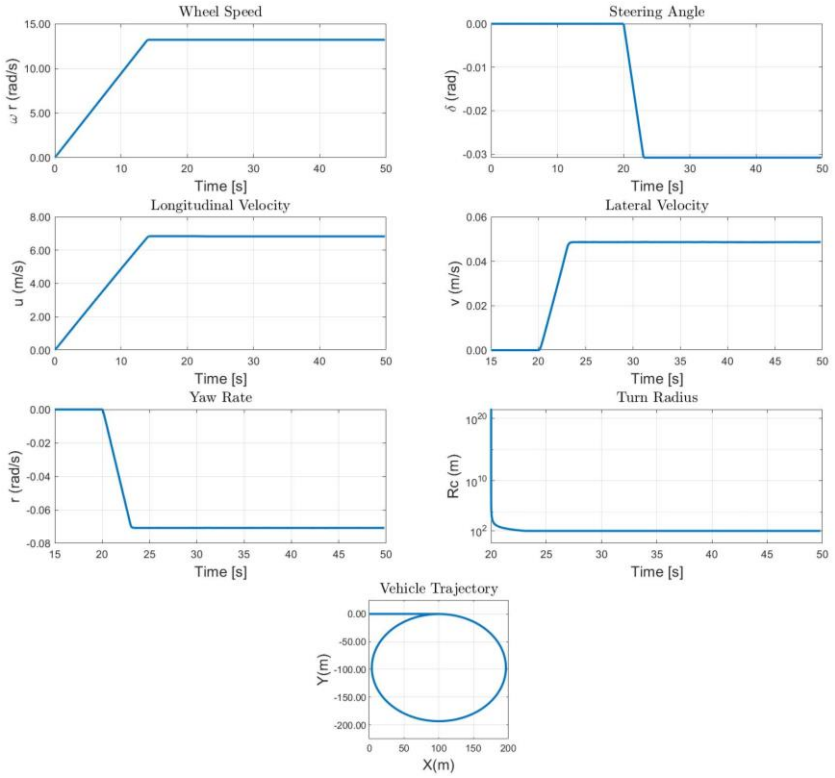

Figure 35. Responses of the Ackerman steered wheeled vehicle for 100 m turn radius at 7 m/s.

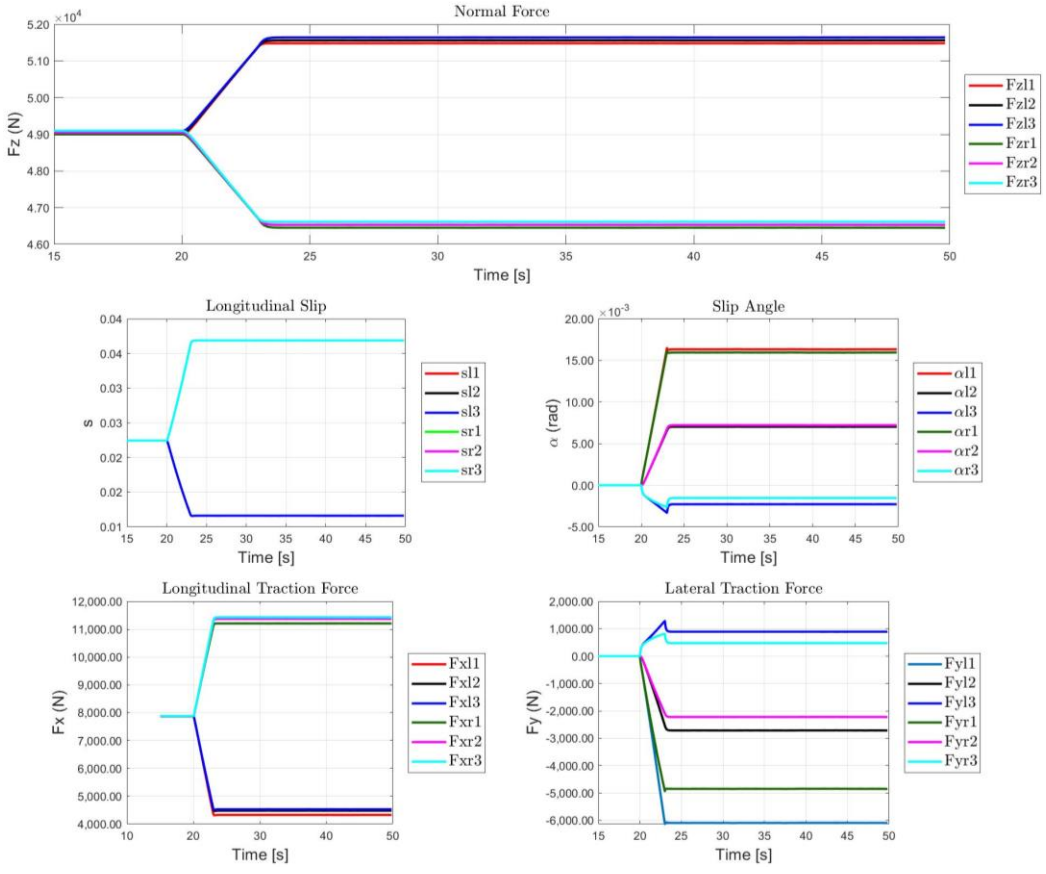

Figure 36. Responses of the Ackerman steered wheeled vehicle for 100 m turn radius at 7 m/s.

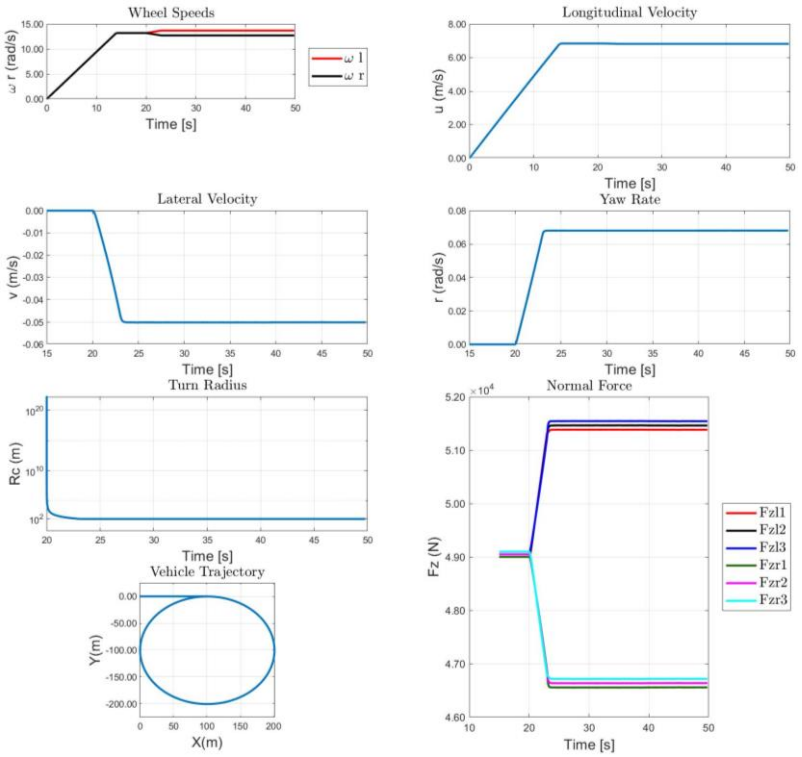

Figure 37. Responses of the skid steered wheeled vehicle for 100 m turn radius at 7 m/s.

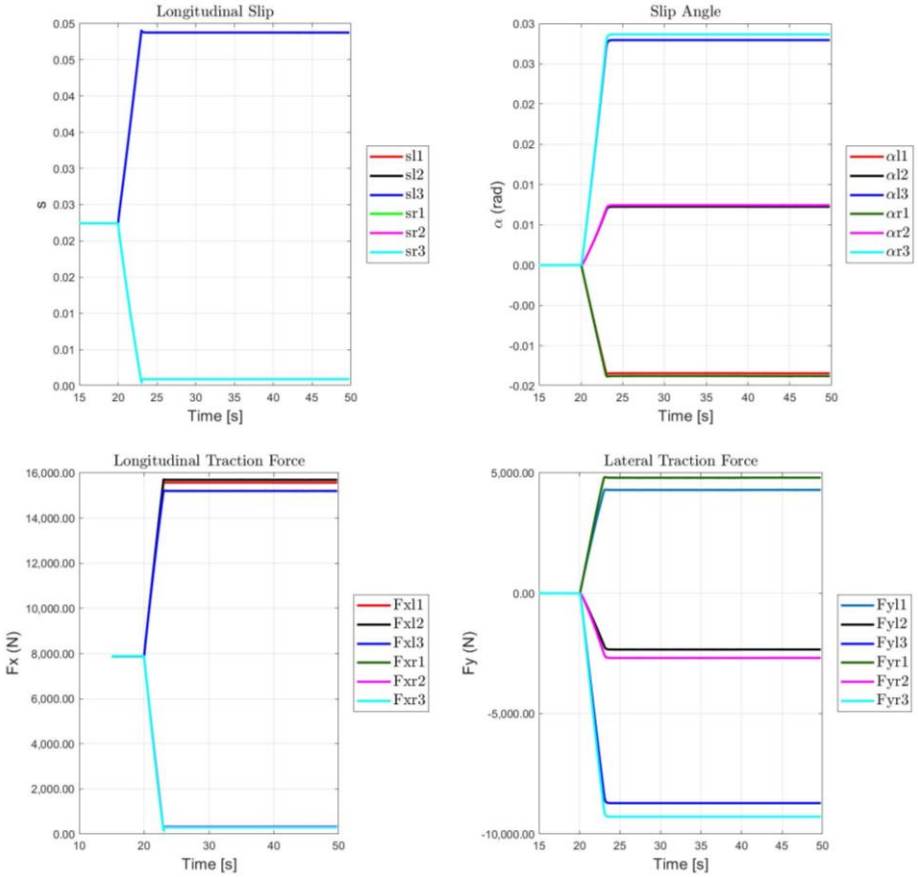

Figure 38. Responses of the skid steered wheeled vehicle for 100 m turn radius at 7 m/s.

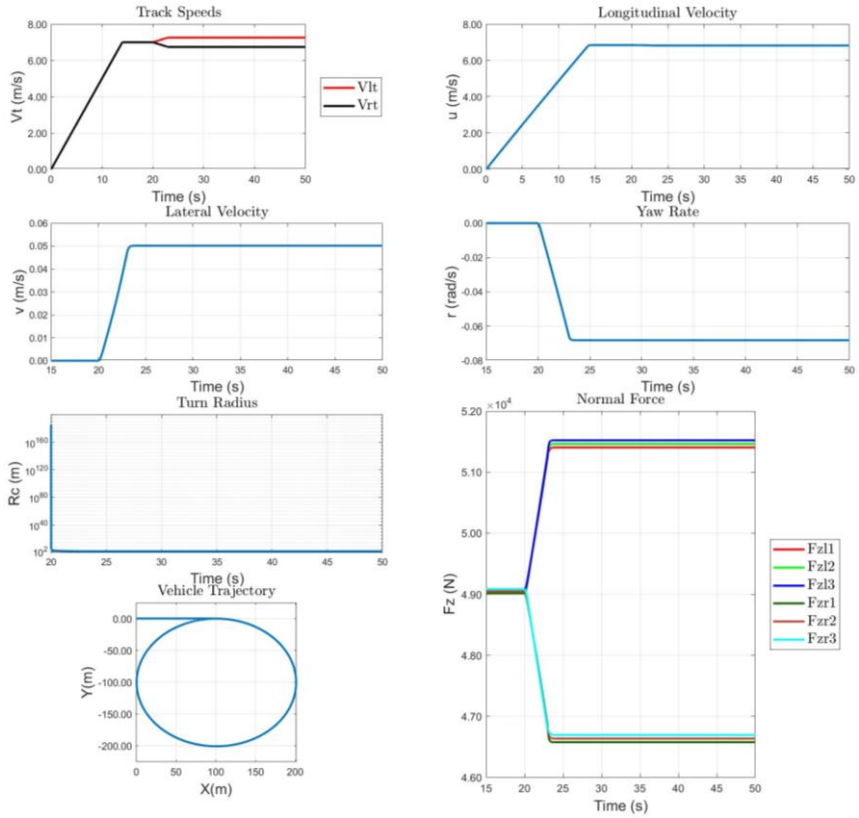

Figure 39. Responses of the six road wheel tracked vehicle for 100 m turn radius at 7 m/s.

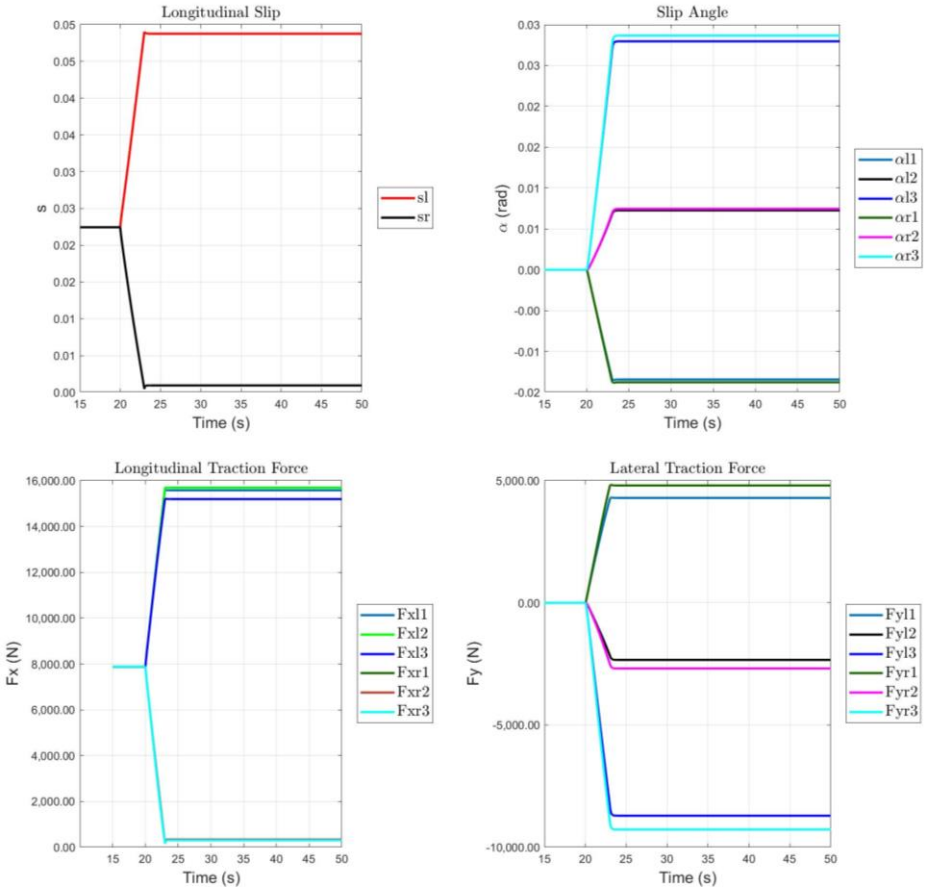

Figure 40. Responses of the six road wheel tracked vehicle for 100 m turn radius at 7 m/s.

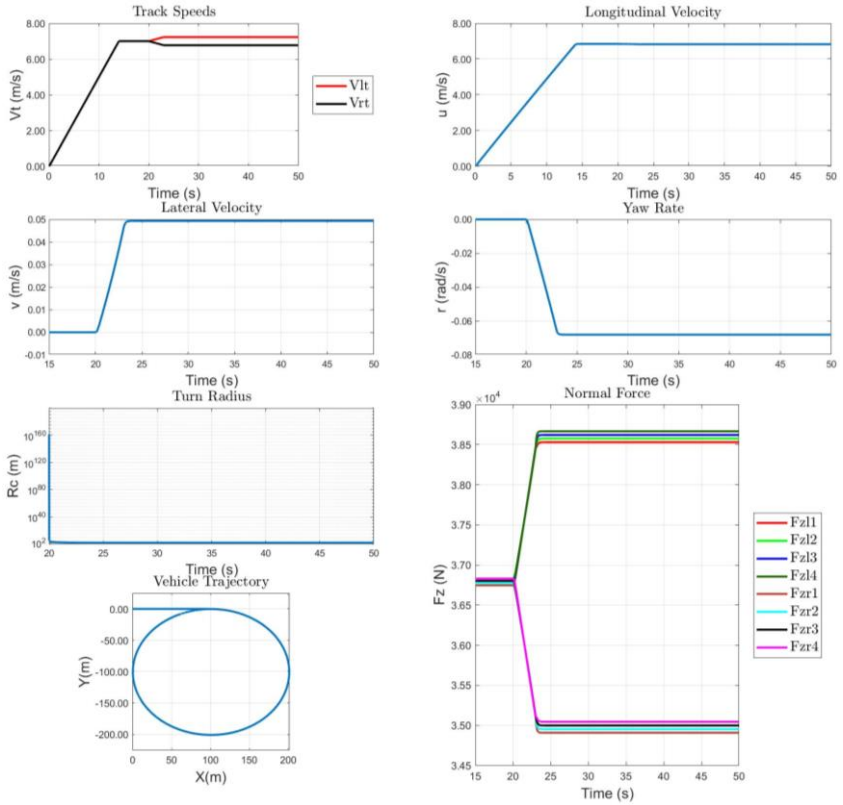

Figure 41. Responses of the eight road wheel tracked vehicle for 100 m turn radius at 7 m/s.

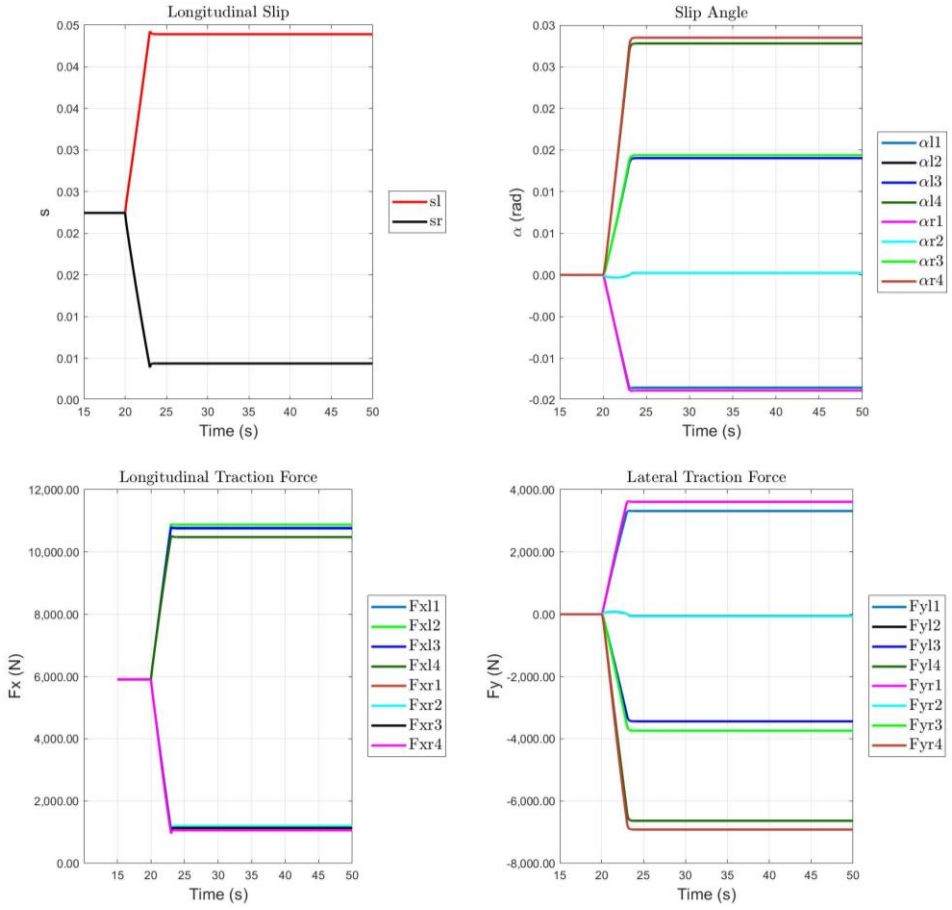

Figure 42. Responses of the eight road wheel tracked vehicle for 100 m turn radius at 7 m/s.

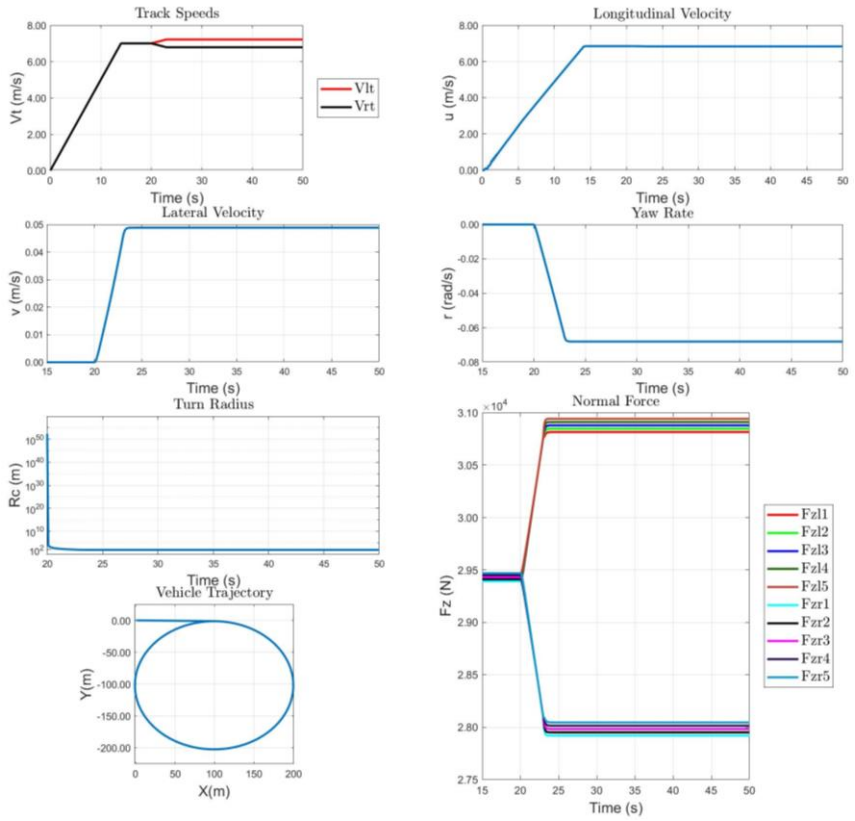

Figure 43. Responses of the ten road wheel tracked vehicle for 100 m turn radius at 7 m/s.

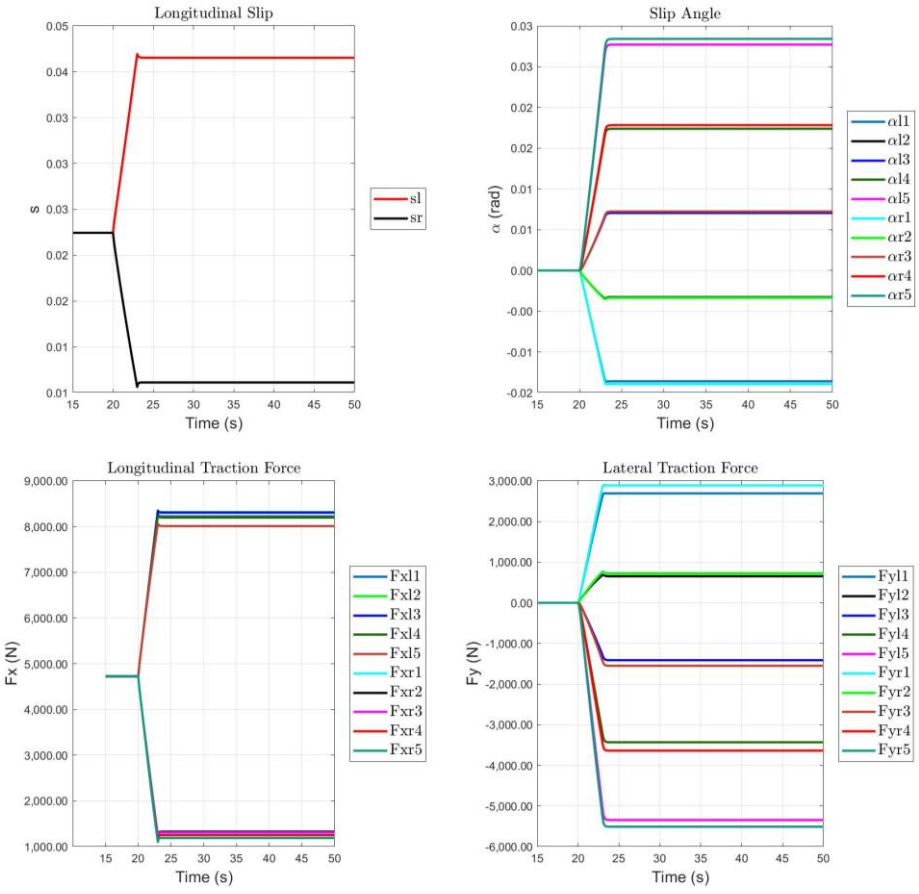

Figure 44. Responses of the ten road wheel tracked vehicle for 100 m turn radius at 7 m/s.

4.4 Steady State Analysis

Steady state analysis is composed of two parts. In the first part yaw rate gain and radius gain responses have been analyzed. Secondly, distributed sprocket torques and lateral coefficient of friction values have been represented with respect to turn radii at different vehicle speeds.

4.4.1 Yaw Rate Gain & Radius Gain

In the Section 4.3, given yaw rate graphs were almost same for all the vehicle types since the turning radii and vehicle speeds were the same. But, yaw rate gain and turning radius gain graphs may give insightful information about the vehicle behavior. To gather these graphs same steering inputs (0.1 for skid steering 0.1 rad for Ackermann steering) applied to all vehicles at varying track or wheel speeds from 1 m/s to 20 m/s.

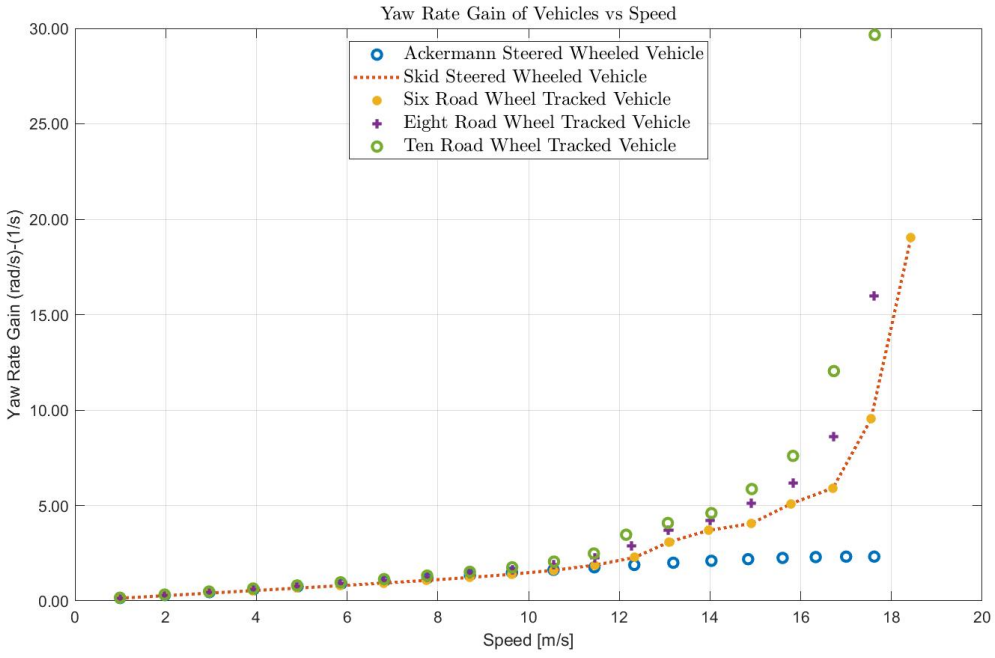

Figure 45. Yaw rate gains of the vehicles.

From the *Figure 45* and *Figure 46* it is clearly seen that skid steering vehicles show rapidly increasing oversteer characteristics after certain points. However, Ackermann

steered wheeled vehicle remains same and shows neutral steer to understeer characteristics under this range of speeds. A more detailed graph can be seen in *Figure 47* where Ackermann steered wheeled vehicle shows understeering behavior after a certain speed.

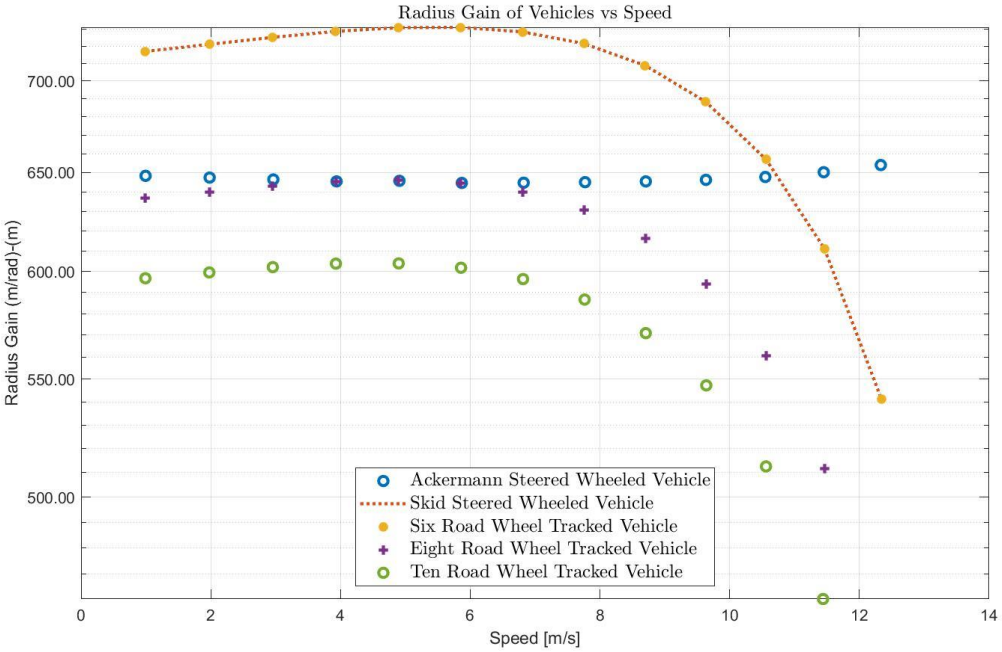

Figure 46. Radius gains of the vehicles.

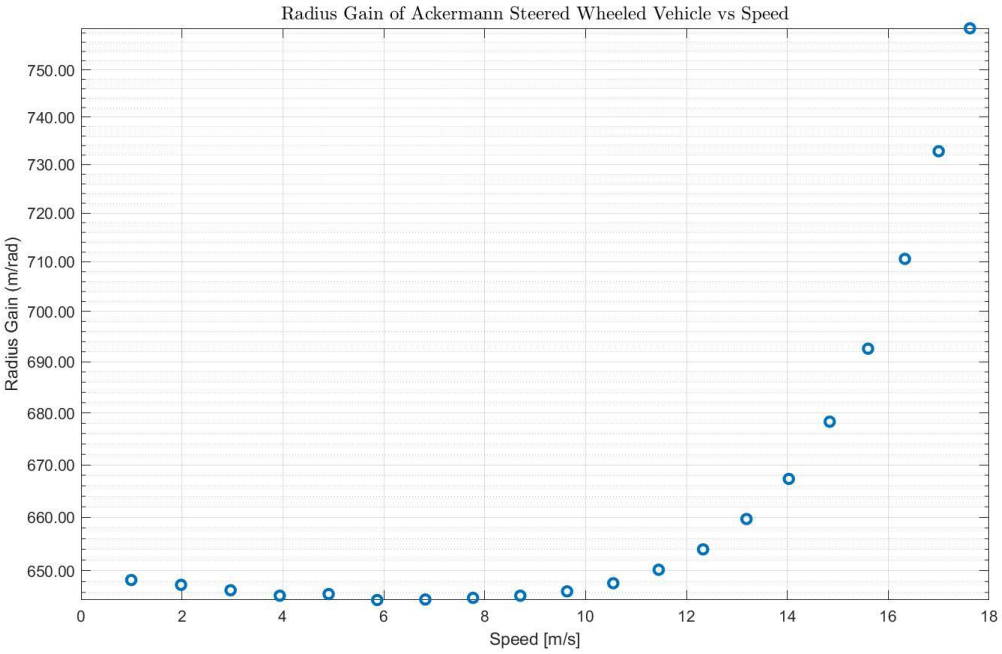

Figure 47. Radius gain of the Ackermann steered wheeled vehicle.

The behavior of the vehicle is related to used ground force generation method. In [1], it has been shown that when Merritt/Steeds coulomb friction based formula is used, in the tracked vehicle exhibits understeering behavior up to certain lateral accelerations (). Conversely, when the flexible pad method is used the same tracked vehicle shows oversteering behavior. Besides, Maclaurin [23] investigated behaviors of Ackermann steered and skid steered wheeled vehicle using a normalized Magic Formula for force generation calculation. Both of the vehicles were same in size and etc. The Ackermann steered vehicle showed understeering behaviors whereas, skid steered vehicle showed oversteering behaviors.

In addition to these, in the flexible pad formula the parameters have been changed for Ackermann steered vehicle. The power of ‘e’ in the formula has been changed from -10.7 to -12 for first axle and -9.4 for third axle. The Ackermann steered vehicle showed oversteering behaviors up to 15 m/s vehicle speeds as seen in *Figure 50*. Both of the vehicle behavior changes, with change in force generation method and with parameter change in the same method, indicates that the behavior of a vehicle in a simulation is affected by the traction force calculation methods and parameters.

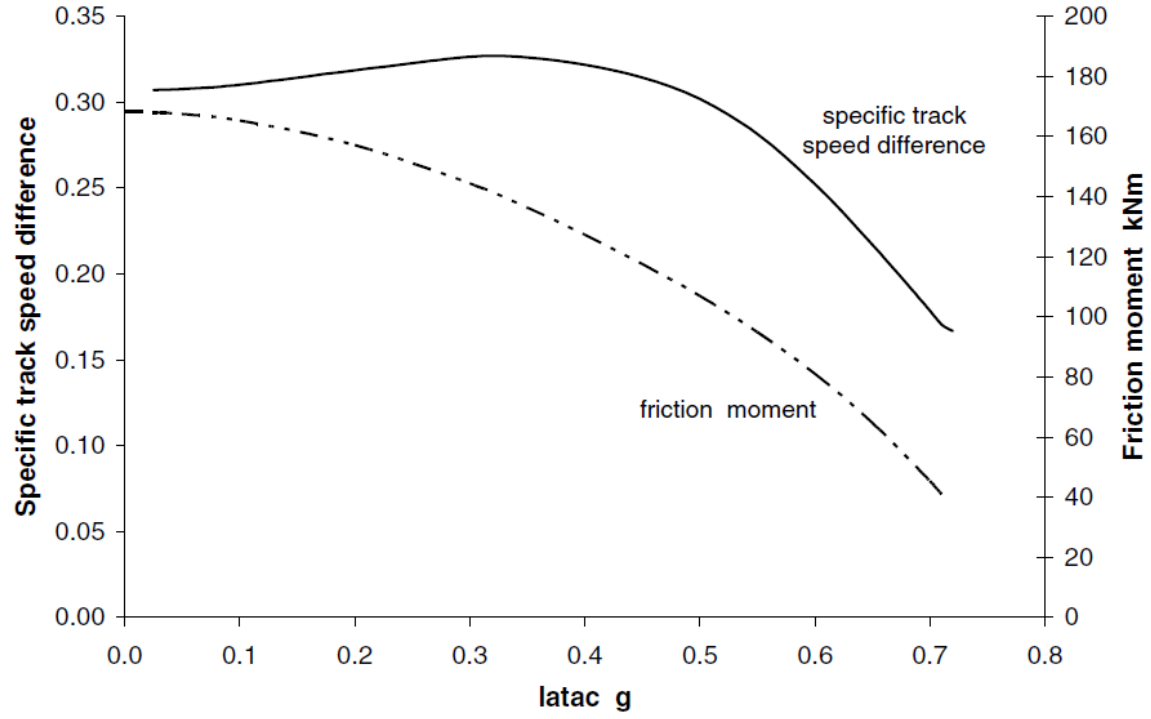

Figure 48 Required track speed difference for a 15 m turn radius at different speeds for a Merritt/Steeds method used vehicle [1].

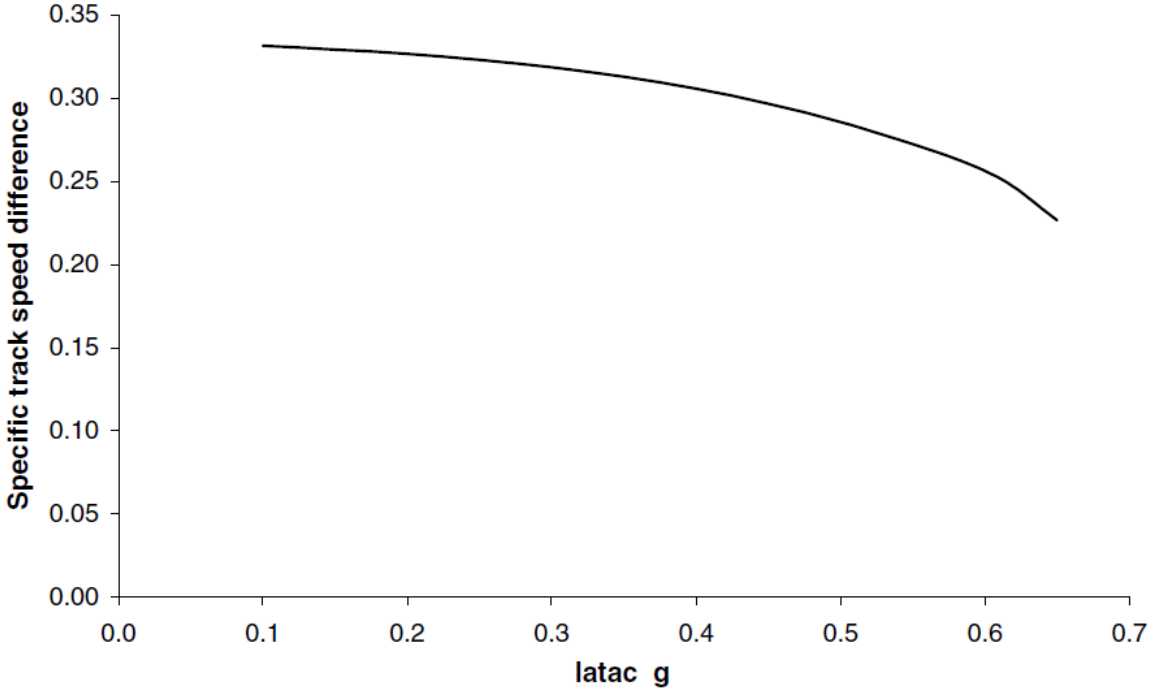

Figure 49 Required track speed difference for a 15 m turn radius at different speeds for a flexible pad method used vehicle [1].

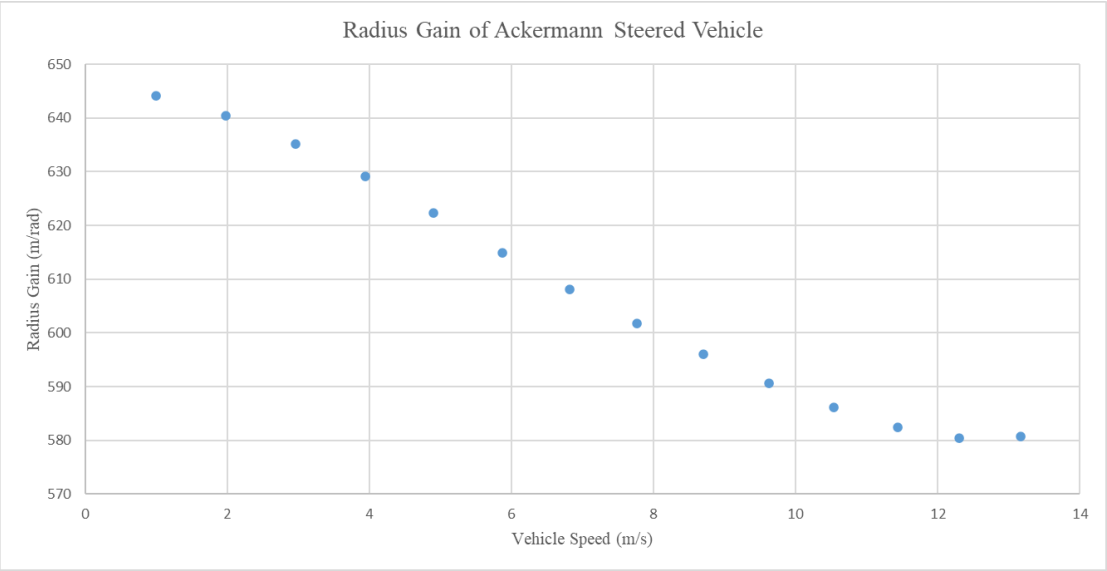

Figure 50 Radius gain of Ackermann Steered vehicle when the power of 'e' in the flexible pad formula is changed to -12 for first axle and -9.4 for third axle.

4.4.2 Sprocket Torques & Lateral Coefficient of Frictions

The sprocket torques for skid steering vehicles have been studied widely for varying turn radii at different vehicle speeds in the literature. It is important to show the general characteristics of the sprocket torque distribution and lateral coefficient resistance to validate the model. Below graphs, represent left and right side torque distributions and lateral coefficient of friction variations of skid steering vehicles for different turn radii at varying speeds.

An example of steering and speed input to the vehicles for above graphs shown below in *Figure 51*. A hundred variants of it have been applied to get different turn radii at various vehicle speeds.

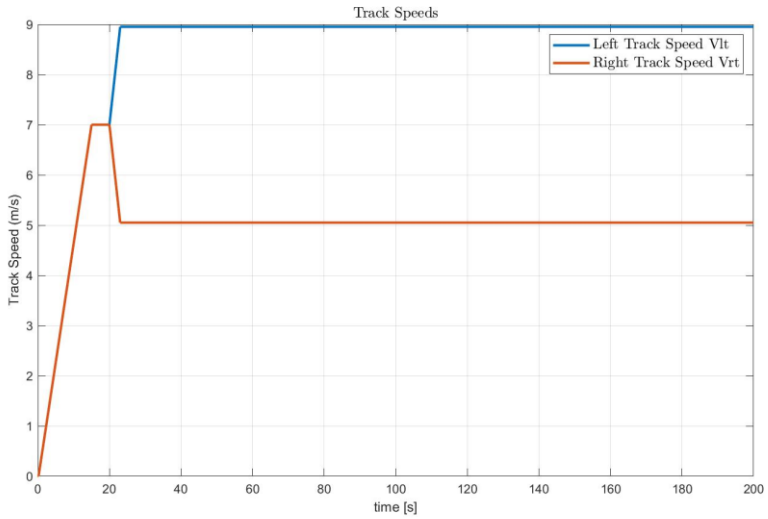

Figure 51. Steering and speed input to the vehicles.

Below, *Figure 52* and *Figure 53* represent sprocket torque distributions and lateral coefficient of friction of six road wheel tracked vehicle at different vehicle speeds and different turn radii. As the radius of turn decreases the required amount of torque increases and at the tighter turns, inner sprocket needs to be braked to accomplish the turn. As the turn radius increases the inner and outer sprocket torques coincide. The lateral coefficient of friction decreases with increasing turn radius and increasing vehicle speed.

All of the skid steering vehicles, that modelled in this thesis, show same behavior for sprocket torque distributions and lateral coefficient of friction variations.

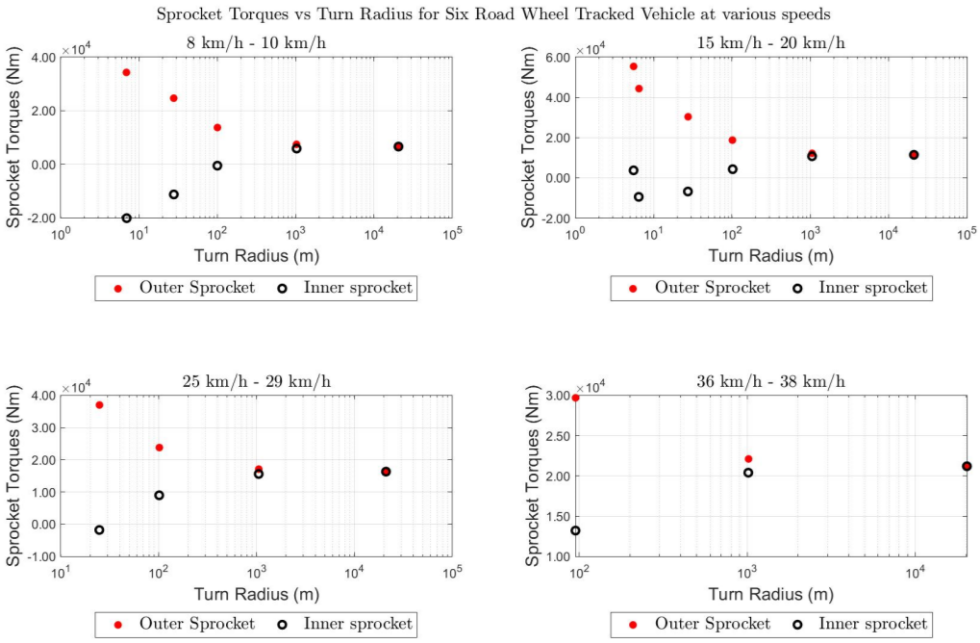

Figure 52. Outer and Inner sprocket torques of the six road wheel tracked vehicle.

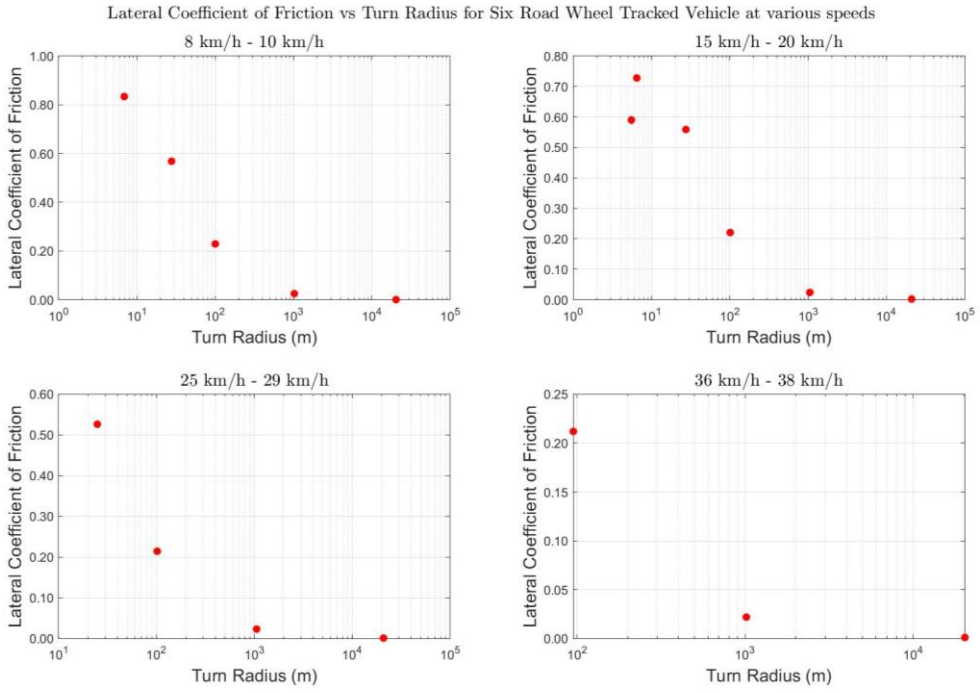

Figure 53. Lateral coefficient of friction of the six road wheel tracked vehicle.

The above results represent general sprocket torque distribution and lateral coefficient of friction change behaviors during various maneuvers of a skid steering vehicle. The consistency of characteristics of these behaviors with the literature [3] shows that the created vehicle models are valid.

5. CONCLUSION

In this thesis, five different vehicle models have been developed for two different wheeled vehicles and three different tracked vehicles. The simulation models have been created in MATLAB SIMULINK. The flexible pad formula has been used to calculate traction forces for all vehicles. Even the flexible pad formula is for tracked vehicles, it has been adopted to work for wheeled vehicles. Combined slip and load transfers due to roll and

pitch motions of the vehicle body have been integrated into models. So that the simulation models are able to calculate complex maneuvers.

The simulation models are capable of executing point turn maneuvers for skid steering vehicles. Results show good agreement with the expectations. Turning radius, lateral and longitudinal velocities resulted zero and no load transfers happened since CG is geometrically symmetric.

The required steering inputs to make constant turn radius maneuvers at different speeds gave insightful information about the nature of the vehicles. Tracked vehicles with more road wheels are advantageous since the vehicle responses are more agile. Required amount of steering input decreases as the number of road wheels increase for the same radius at the same speed. Another outcome is that skid steering vehicles show oversteer behaviors while the Ackermann steered vehicle shows understeer behaviors for this thesis parameters set.

6. FUTURE WORKS

In the scope of this thesis extensive simulation studies have been conducted. This kind of highly concentrated simulation containing theses have many subjects to be improved. Some of them have been discussed below.

In the scope of this thesis only firm ground is used. There are various kinds of terrains on which both tracked and wheeled vehicles may operate. For example, when a soft clay terrain or a muddy terrain included to the models, all of the traction force generation

mechanics change. The sinking of the vehicles, bulldozing effects and other considerations have to be analyzed. Therefore, the work done in the scope of this thesis can be improved by including other types of terrains.

The traction force generation method used is the flexible pad method of Maclaurin [1]. There are other methods as described in the literature review sections. They can be also adopted and used in the models.

The mathematical vehicle models do not include suspension geometries. A more detailed model can be created including suspension geometry details like camber, caster and toe angles etc. As the detail of the model increases the simulations approach to reality. But, as the detail of the model increases the complexity of the solution increases and it is becoming hard to handle the models.

6. REFERENCES

[1] B. Maclaurin, A skid steering model with track pad flexibility, Journal of Terramechanics, 44(1) **(2007)** 95-110.

[2] E. Galvagno, E. Rondinelli, M. Velardocchia, Electro-mechanical transmission modelling for series-hybrid tracked tanks, International Journal of Heavy Vehicle Systems, 19(3) **(2012)** 256.

[3] J.Y. Wong, C.F. Chiang, A general theory for skid steering of tracked vehicles on firm ground, Proceedings of the Institution of Mechanical Engineers, Part D: Journal of Automobile Engineering, 215(3) **(2001)** 343-355.

[5] K. Bayar, Modelling of the Dynamics of Multi-Axle Steered Vehicles, Master Thesis, The Graduate School of Natural and Applied Sciences of Middle East Technical University, Ankara, **2006**

[6] J. Ni, J. Hu, X. Li, Dynamic modelling, validation and handling performance analysis of a skid-steered vehicle, Journal of Automobile Engineering, 230(4) **(2015)** 514-526.

[7] R.N. Jazar, Vehicle Dynamics Theory and Application, Springer, Cham, **2018,**

[8] H.B. Pacejka, Tyre and Vehicle Dynamics, Elsevier Butterworth-Heinemann, Amsterdam, **2009**,

[9] M. Kitano, M. Kuma, An analysis of horizontal plane motion of tracked vehicles, Journal of Terramechanics, 14(4) **(1977)** 211-225.

[10] E. Bakker, L Nyborg, H.B. Pacejka, Tyre modelling for use in vehicle dynamic studies, SAE Technical Paper 870432 **(1987)**.

[11] H. Dugoff, P.S. Fancher, L. Segel, An analysis of tire traction properties and their influence on vehicle dynamic performance, SAE paper 700377 **(1970)**.

[12] H.B. Pacejka, E. Bakker, The magic formula tyre model, Vehicle System Dynamics: International Journal of Vehicle Mechanics and Mobility, 21(S1) **(1992)** 1-18.

[13] W. Steeds, Tracked Vehicles, Automobile Engineer, 40(4) **(1950)** 143.

[14] J.Y. Wong, Theory of Ground Vehicles, John Wiley, New York, **2000**,

[15] J.Y. Wong, Terramechanics and Off-Road Vehicles, Elsevier, Amsterdam and New York, **1989**,

[16] W. Ehlert, B. Hug, I.C. Schmid, Field measurements and analytical models as a basis of test stand simulation of the turning resistance of tracked vehicles, Journal of Terramechanics, 29(1) **(1992)** 57-69.

[17] J. Hock, Lenkgetriebe für Kettenfahrzeuge, Firmenschrift, ZF Friedrichshafen,

(1970).

[18] M. Kitano, H. Jyozaki, A theoretical analysis of steerability of tracked vehicles, Journal of Terramechanics, 13(4) **(1976)** 241-258

[19] W. Ehlert, Simulation der Fahrwiderstände von Gleiskettenfahrzeugen auf dem Prüfstand, insbesondere bei Kurvenfahrt, Universität der Bundeswehr Hamburg, **(1991)**.

[20] B. Maclaurin, A skid steering model using Magic Formula, Journal of Terramechanics, 48(4) **(2007)** 95-110.

[21] M. Garber, J.Y. Wong, Prediction of ground pressure distribution under tracked vehicles-I, Journal of Terramechanics, 14(4) **(1981)** 1-23.

[22] M. Abe, Vehicle handling dynamics: Theory and application, Elsevier Butterworth-Hein, Oxford, **2015**,

[23]B. Maclaurin, Comparing the steering performances of skid and Ackermann steered vehicles, Proceedings of the Institution of Mechanical Engineers, Part D: Journal of Automobile Engineering, 222 (5) **(2008)** 739-756